

UNIVERSITY OF TARTU

Faculty of Science and Technology

Institute of Ecology and Earth Sciences

Martin Mäll

**MODELLING STORM SURGE CONDITIONS UNDER FUTURE  
CLIMATE SCENARIOS: A CASE STUDY OF 2005 JANUARY STORM  
GUDRUN IN PÄRNU, ESTONIA**

Master thesis in Environmental Technology (30 EAP)

Supervisors: PhD Ülo Suursaar

PhD Ain Kull

Prof. Tomoya Shibayama

Tartu 2016

## **Modelling storm surge conditions under future climate scenarios: A case study of 2005 January storm Gudrun in Pärnu, Estonia**

Extra-tropical cyclones induced coastal disasters are the most dangerous natural hazards in the Baltic Sea region. Understanding how these storms behave in the future is of high importance to decision makers and risk management groups. Atmospheric and ocean models were backtested against 2005 Gudrun observational data. From there on background forcing conditions were modified to evaluate the possible “future Gudrun” effects at Pärnu. Future simulations were based on MIROC5 data for 2050 and 2100, considering projections for RCP4.5 and RCP8.5 scenarios. Hindcast results showed good agreement with observations. Future storms did not show any intensification, which is believed to be due to the mechanism of such storms. Further research with improved methodology is needed to reduce uncertainty.

Keywords: *extra-tropical cyclones, storm surge, future projections, models, Baltic Sea*

P500 Geophysics, physical oceanography, meteorology

## **Tulevikutormide simuleerimine, kasutades atmosfääri- (WRF) ja ookeanimudelit (FVCOM) 2005. aasta jaanuaritormi (Gudrun) näitel**

Parasvöötme tsükloneid peetakse Läänemere piirkonnas ohtlikemaiks loodus katastroofideks. Sellest tulenevalt on oluline paremini mõista tulevikus esineda võivaid torme ja nende mõjusid Eesti kontekstis. Atmosfääri ja ookeani mudeli valideerimiseks teostati järelanalüüs 2005. a Gudruni kohta. Tulevikustsenariumite saamiseks kasutati MIROC5 poolt manipuleeritud andmeid aastatele 2050 ja 2100, arvestades RCP4.5 ja RCP8.5 stsenaariumitel põhinevaid projektsioone. Järelarvutuse tulemused olid heas kooskõlas mõõdetud andmetega. Muudetud parameetritega „tuleviku Gudrunid“ ei muutunud tugevamaks. Peamiseks põhjuseks võib pidada parasvöötme tsüklonite arengu eripära. Kuid ühest tulevikutormi arvutustulemusest ei piisa klimatoloogiliste üldistuste tegemiseks. Seetõttu on oluline täiendada olemasolevat metoodikat ja arvutada läbi erinevate trajektooridega ja eri aastaaegadel asetleidvaid torme.

Märksõnad: *parasvöötme tsüklonid, üleujutused, tuleviku projektsioonid, mudelid, Läänemeri*

P500 Geofüüsika, füüsikaline okeanograafia, meteoroloogia

## Contents

1	Introduction .....	4
2	Material and Methods.....	6
2.1	Material .....	6
2.2	Methods.....	9
2.2.1	General framework .....	9
2.2.2	WRF.....	9
2.2.3	FVCOM.....	11
2.2.4	Hindcast .....	12
2.2.5	Future simulations .....	13
3	Results and Discussion .....	15
3.1	Description of met-ocean conditions during the historic storm Gudrun .....	15
3.2	Hindcast results .....	16
3.3	Projections of extratropical-cyclones according to Global Climate Models.....	24
3.4	Characteristics of storm Gudrun under future climate change scenarios.....	25
3.4.1	Wind speed .....	28
3.4.2	Wind direction .....	29
3.4.3	Surge height.....	30
3.4.4	Standard deviation of wind speed.....	31
3.5	Final remarks and proposals for further research.....	34
4	Conclusions .....	35
	Acknowledgements.....	39
	References.....	40
	Appendices.....	46

# 1 Introduction

Presently the increase in storminess is considered to be one of the most dangerous offshoots of climate change, which with the global sea level rise threatens many low-lying populated coastal areas such as Netherlands, Southeast Asia, Gulf of Mexico region etc (Emanuel, 2005). The projected rise of global sea surface temperature might be thought to cause the intensification of tropical- and extra-tropical cyclones. However some researchers believe it yet to be as resolute (Schmidt & von Storch, 1993; Trenberth, 2005), due to the high natural variability of cyclogenesis (Rutgersson et al., 2015). In addition, the increasing negative impacts to human lives and economy might not only reflect the trend in increase of storminess as a geophysical occurrence but also the constant growth of population and economic enterprises in the coastal zones. Moreover, the increase in storminess is certainly not a uniform and all-encompassing phenomenon (Feser et al., 2014).

The mechanism of cyclogenesis is different from that in the tropics and in the mid-latitudes. Also their nature, parameters and effects differ. Strong tropical cyclones (hurricanes, typhoons), such as Katrina (2005, Gulf of Mexico), Nargis (2008, Bay of Bengal), Sandy (2012, East Coast USA), Hayian/Yolanda (2013, Phillipines), have had the biggest influence in the recent decade. The effect of these storms have been studied by a number of research groups (Hill, 2012; Nakamura et al., 2015a,b; Shibayama, 2015) by utilizing various models and initial conditions as well incorporating ones that allow to shed some light to questions such as how the „future Hayian“ or „future Nargis“ might be perceived?

Climate change related hazards, such as increase in storminess and flooding, might also have an effect on the Baltic Sea region (Avotniece et al., 2010; Suursaar et al., 2015). The threat level increase is partly due to the fact that the steady increase in global sea level rise has so far been compensated by the post-glacial rebound in the northern and eastern areas of the Baltic Sea. However, this effect is slowly weakening, mainly because of global sea level rise and its probable acceleration. According to the latest IPCC's (Intergovernmental Panel on Climate Change) Fifth Assessment Report (AR5), global mean sea level (GMSL) has risen by 0.19 [0.17 to 0.21] m over the period 1901–2010; it is very likely that the mean rate increased to 3.2 [2.8 to 3.6] mm yr<sup>-1</sup> between 1993 and 2010. For the period 2081–2100, compared to 1986–2005, and following the IPCC's Representative Concentration Pathways (RCP's), the GMSL is likely to be 0.26 to 0.55 m for RCP2.6, 0.32 to 0.63 m for RCP4.5, 0.33 to 0.63 m for RCP6.0, and 0.45 to 0.82 m for RCP8.5. For RCP8.5, the rise by 2100 is 0.52 to 0.98 m

with a rate during 2081–2100 of 8 to 16 mm yr<sup>-1</sup>. Consequently, even if the storms would retain their strength throughout the 21th century, mild storm surges still become severe and severe ones turn to catastrophic. However, storm pathways may change in time (e.g. Sepp et al., 2005; Pinto et al., 2007) and also, future storms may become more frequent and stronger.

Therefore, from the view of climatic aspects, the extra-tropical cyclones (ETC) pose the greatest threat to the Baltic Sea region. Such atmospheric low pressure systems form near the polar front in the Northern Atlantic Ocean, between Iceland, Greenland and Newfoundland Peninsulas, during the colder half of the year. While moving along the westerlies towards the Baltic Sea region, these ETC-s can pose great threat for the British Isles, Scandinavia and other parts of Northern Europe (Post & Kõuts, 2014). According to the Extreme Wind Storms (XWS) Catalogue (Roberts et al., 2012), the most influential storms in Western Europe of the past few decades have been 87J (October 1987), Daria (January 1990), Vivian (February 1990), Anatol (December 1999), Gudrun/Erwin (January 2005) and Cyril (January 2007). However true, different meteorological indexes give somewhat dissimilar results. The north-south extent of the Baltic Sea is quite considerable (approx. 1400 km) and the local storm effect highly depends on the storm trajectory. Therefore the list of most influential historical storms in the Estonian coastal waters slightly differs (Jaagus & Suursar, 2013; Suursaar et al., 2015): Gudrun/Erwin (9th January 2005), storms on 2nd November 1969, 18th October 1967, 17th December 1990, 1st November 2001, 22nd February 1990 and St. Jude (29th October 2013). Of the listed storms, the most extreme storm was the 2005 January Storm Gudrun, which invoked storm surge caused record high flooding in various coastal cities. The tide gauge in the mouth of the river Pärnu recorded +275 cm sea level rise above the mean value. This historical storm and its invoked storm surge caused major economic loss and coastal damage (Suursaar et al., 2006; Tõnisson et al., 2008).

Considering the evident storm damage during the past decades and the likely impending climate change, it is necessary to better understand the storms of the future in the context of Estonia. Will the ETCs under the rising temperatures become stronger in the Baltic Sea region? Will the flooding caused by the storm surges become more intensive due to the global sea level rise (Eelsalu et al., 2014)? The aim of this study is to reconstruct the historical storm Gudrun by means of Advanced Research Weather Research and Forecasting (ARW-WRF) model and Finite Volume Community Ocean Model (FVCOM). „Future Gudruns“ are simulated for years 2050 and 2100 in accordance with IPCC AR5 proposed RCP4.5 and RCP8.5 climate change scenarios (Collins et al., 2013).

## **2 Material and Methods**

### **2.1 Material**

#### **Meteorological data**

7 meteorological stations were used to assess the quality of atmospheric model results. The following meteorological stations were used: Ruhnu, Kihnu, Sõrve, Vilsandi, Virtsu, Ristna and Pärnu-Sauga. Figure 1 shows the location and nearby surrounding of these stations. Meteorological parameters like wind speed and direction were used from a period of 18:00 UTC 06/01/2005 – 18:00 UTC 10/01/2005, provided by the Estonian Weather Service.

The measured storm track data, following the minimum sea level pressure (MSLP), of 2005 storm Gudrun was acquired from Extreme Wind Storms (XWS) Catalogue.

#### **Water level data**

Water level measurements from Pärnu tide gauge were used to assess the quality of ocean model results. The water level data was used from a period of 06:00 UTC 08/01/2005 – 12:00 UTC 10/01/2005, provided by the Estonian Weather Service.

#### **Atmospheric model input data**

NCEP FNL Operational Global Analysis (NCEP FNL, 2000) 6-hourly GRIB-formatted meteorological data with 1-degree by 1-degree grids was used to generate the meteorological conditions. The data consists of 27 variables and was used from a period of UTC 06/01/2005 – 18:00 UTC 10/01/2005, provided by the US National Centers for Environmental Prediction.

For future simulations three selected variables, considering RCP4.5 and RCP8.5 scenarios, from MIROC5 global climate model were averaged and interpolated to existng NCEP FNL produced metgrids. These variables include: atmospheric air temperature, sea surface temperature and relative humidity. Variables data was acquired from a period of January 2006-2011, January 2045-2055 and January 2091-2100 representing control period, year 2050 and year 2100, respectively.



**Figure 1.** Location and surroundings of 7 selected meteorological stations.

### Ocean model input data

Output data from atmospheric model was an input data for the ocean model in order to simulate the water levels. Bathymetry with 3 different spatial resolutions was used – high resolution data with 5 m was used for the Pärnu Bay and river; 50 m for the Gulf of Riga, Väinameri and Irbe Straight, provided by Estonian Maritime Administration; lower resolution data of 1 arc-minute covered rest of the study area, provided by ETOPO1. Coastline elevation with 3 different resolutions was used – high resolution data with 5 m DEM LIDAR was used for Pärnu city, provided by the Estonian Land Board; 90 m resolution data was used for the Pärnu Bay, provided by SRTM90; low resolution data of 1 arc-minute was used for the rest of the study area, provided by ETOPO1 (Table 1).

**Table 1.** Initial and boundary conditions for used models

	List	Options and schemes
WRF	Simulation time (domain 1)	18:00 UTC 06/01/2005 – 18:00 UTC 10/01/2005
	Simulation time (domain 2)	06:00 UTC 07/01/2005 – 18:00 UTC 10/01/2005
	Simulation time (domain 3)	06:00 UTC 08/01/2005 – 18:00 UTC 10/01/2005
	Grid resolution (domain 1)	22.5 km
	Grid resolution (domain 2)	4.5 km
	Grid resolution (domain 3)	0.9 km
	Pressure top	50 hPa
	Vertical layers	27
	Number of domains	3
	Nesting scheme	2-way nesting
	Micro physics	WSM6 (Hong and Lim, 2006)
	Surface layer	Revised MM5 Monin-Obukhov scheme (Paulson, 1970; Dyer and Hicks 1970; Webb, 1970; Beljaars, 1994; Zheng and Anthes, 1982) and Hicks 1970; Webb, 1970; Beljaars, 1994; Zheng and Anthes, 1982)
	Land surface option	Unified Noah land-surface model (Tewari et al., 2004)
	Planetary boundary condition	YSU (Hong et al., 2006)
	Map projection	Lambert conformal
FVCOM	Bathymetry data	USGS
	Meteorological data	NCEP FNL Operational Global Analysis
	Meteorological data resolution	1 x 1 °
	Simulation time	06:00 UTC 08/01/2005 – 12:00 UTC 10/01/2005
	Nodes	63 189
	Cells	123 533
	Mesh size	50 m – 2000 m
	Coastline data (Estonian Land Board)	Pärnu city - 5 m (DEM LIDAR)
	Coastline data (SRTM90)	Pärnu Bay - 90 m
	Coastline data (ETOPO1)	Rest of the study area - 1 arc-minute
	Bathymetry data (Estonian Maritime Administration)	Pärnu Bay and river - 5 m; Gulf of Riga, Väinameri and Irbe Straight - 50 m
	Bathymetry data (ETOPO1)	Rest of the study area - 1 arc-minute

## 2.2 Methods

### 2.2.1 General framework

The modelling system and the methodology used for modelling the atmospheric and storm surge conditions is depicted in Figure 2 (after Nakamura et al., 2015b). Top-down approach was adapted for simulations, where the atmosphere model is ran first and the output is used as an input for the ocean model. Similar framework has also been used in studies by Tasnim et al. (2015), Nakamura et al. (2015a,b; 2016). Detailed information of initial and boundary conditions, as well as chosen modelling schemes, are presented in Table 1.

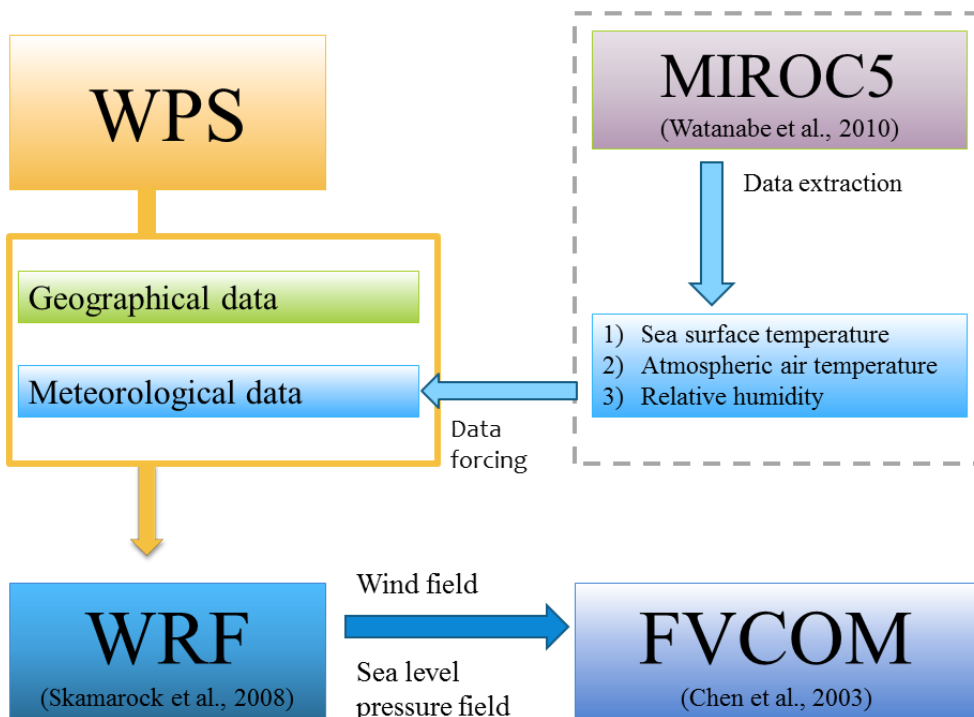


**Figure 2.** Flowchart of models used for storm surge modelling

### 2.2.2 WRF

The Weather Research and Forecasting (WRF) Model is a mesoscale numerical weather prediction model. The WRF model has a wide variety of physics packages and modules which can be applied for many different fields of study. WRF coupled with Chemistry (WRF-Chem) for instance can be used to investigate regional scale air quality. A wildland fire module, WRF-Fire, can be used to model the growth of wildland fire.

The development efforts of WRF began at the late 1990s as part of collaborative partnership between a number of institutes (NCAR, NOAA, AFWA, NRL etc.) and universities (e.g. The University of Oklahoma). The model has a wide users community with already over 30 000 registered users in more than 150 countries. The WRF has two dynamical solvers known as NMM (Nonhydrostatic Mesoscale Model) and ARW (Advanced Research WRF) core, thus being able to generate atmospheric simulations with idealized conditions or using real data (Skamarock et al., 2008). WRF version 3.5.1 was used in this study. 2-way nesting scheme was adopted to create 3 domains (Figure 3) of which the third domain covers the western coastline of mainland Estonia and its archipelago system, consequently forming the main study area.

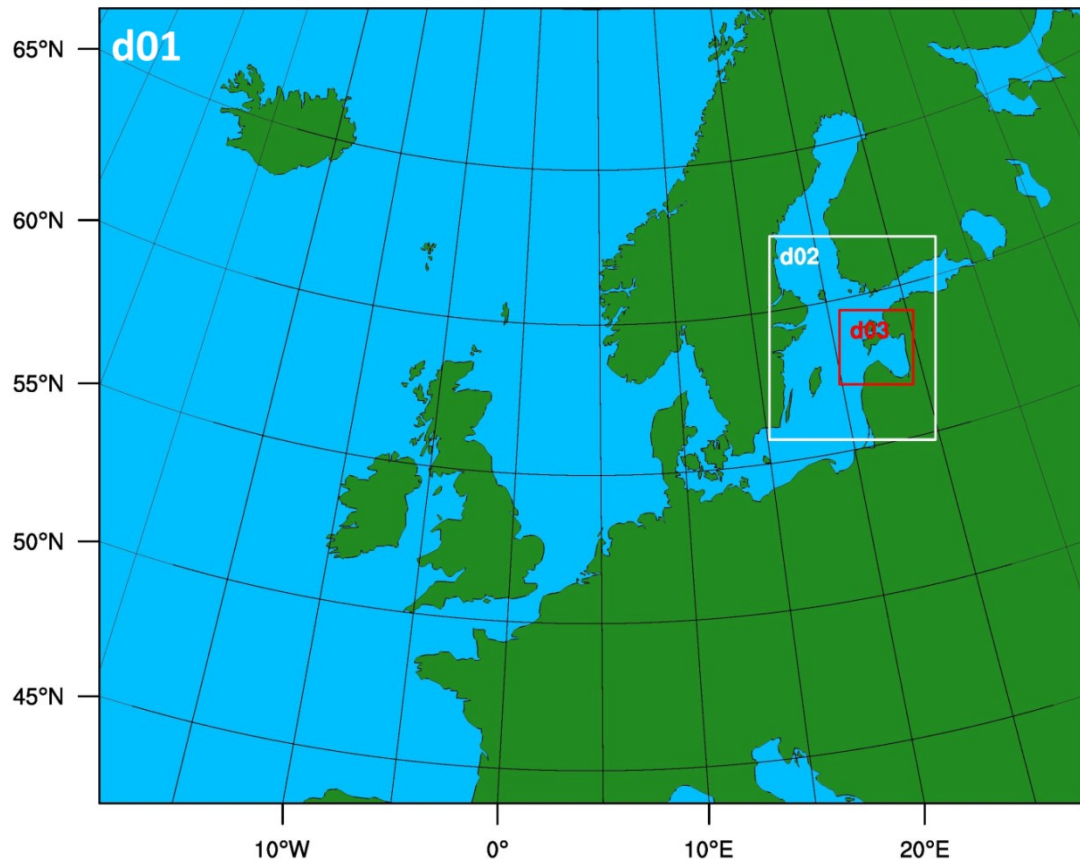


**Figure 3.** Nested domains used in WRF atmospheric model.

The simulation run-time covers the entire significant lifespan of the ETC. Domain one ran for 96 hours, domain two for 84 hours and domain three for 60 hours. Simulation based cyclone tracks were subtracted with Generic Mapping Tool following the atmospheric MSLP. The best track (also, “observed”) MSLP for comparison, was acquired from the Extreme Wind Storms (XWS) Catalogue.

### 2.2.3 FVCOM

Storm surge simulations were conducted using The Unstructured Grid Finite Volume Community Ocean Model (FVCOM) which is a prognostic, unstructured-grid, finite-volume, 3-D primitive equation coastal ocean circulation model. The development of FVCOM was a joint effort of The University of Massachusetts School of Marine Science and Woods Hole Oceanographic Institute (Chen et al., 2003). FVCOM combines the most advantageous parts from finite-difference method and finite-element methods for computational efficiency and for geometric flexibility, respectively.

FVCOM's ability to accurately solve scalar conservation equations and its topological flexibility make it a valuable tool for a variety of coastal and scientific purposes (Chen et al., 2003). The simulated FVCOM domain falls under WRF domain 3 (Figure 4). The simulation run-time for FVCOM was 54 hours, where the main variables affecting the storm surge were

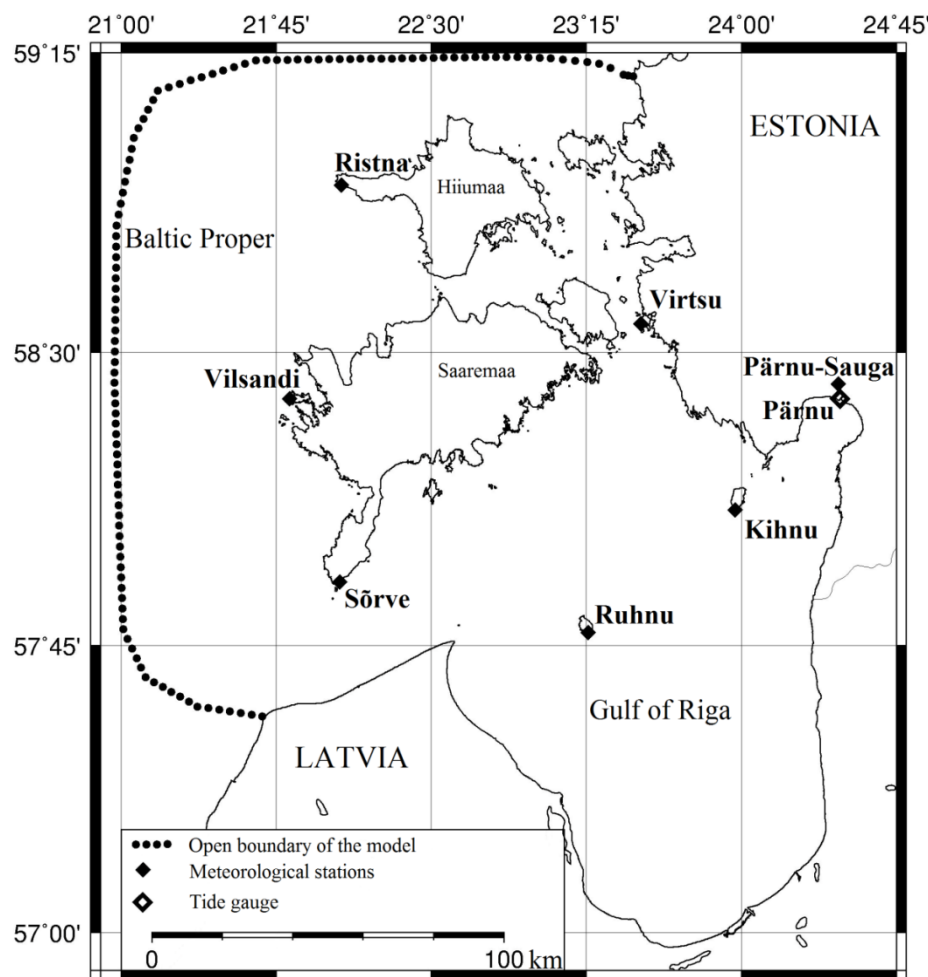


**Figure 4.** FVCOM ocean model study area, which falls under the WRF domain 3 (Figure 3).

the WRF generated wind and air pressure fields. In order to be able to use FVCOM, the preparation of bathymetry and coastline data as unstructured grids was necessary. To achieve this, hydraulic modelling software packages were used: BlueKenue and Surface-water Modelling System (SMS). The Baltic Sea background water level prior to the storm was approximately 70 cm above the mean value (Suursaar et al., 2006). Therefore this condition was also applied for FVCOM model calculations.

## 2.2.4 Hindcast

In order to proceed with future scenario simulations it was necessary to conduct a hindcast (Base case) of the historical Gudrun. For this, the observational data with 1-hourly time-step for wind speed, wind direction from seven meteorological stations and storm surge height from the Pärnu tide gauge was collected. The observational data was compared against WRF and FVCOM output data, where the values of wind speed, direction and surge height were picked from the closest nodes corresponding to the coordinates of the meteorological stations and the tide gauge (see Figure 1&4). Data visualization and variables point extraction was done with VisIt software version 2.9.2. WRF gives u and v wind components at a 10 m height. Therefore wind speed was calculated as follows:

$$Ws = \sqrt{u^2 + v^2} \quad (1)$$

And wind direction with respect to true north

$$Wd = \text{atan2}(u, v) * (180/\pi) + 180 \quad (2)$$

To further evaluate the model output against the observed data, a statistical interpretation is required. To achieve this, three parameters were applied – root mean square error (RMSE), coefficient of determination ( $R^2$ ) and bias. RMSE is the square root of the variance of the residuals and shows the absolute fit of the model to the observed data points thus indicating how close the observed and predicted values are. RMSE gives same units as response variables and is an important criterion to evaluate models prediction. Lower values indicate a better fit.  $R^2$  on the other hand shows the relative measure of fit on the scale of 0 – 1, where 1 is a perfect fit and 0 shows that the regression line does not fit the data at all.  $R^2$  is the squared value of Pearson product moment correlation coefficient  $r$ . The purpose of bias is to determine the error in an estimator and through that showing whether the modelled values have the tendency to be over- or underestimated. It is assumed that if the model is competent

in describing the present climatic conditions then it also capable in giving feasible projections of the future conditions. The formulas for these statistical parameters are as follows:

$$RMSE = \sqrt{\frac{1}{n} \sum (x_i - y_i)^2} \quad (3)$$

$$Bias = \frac{1}{n} \sum (x_i - y_i) \quad (4)$$

$$R^2 = \left( \frac{\sum (x - \bar{x})(y - \bar{y})}{\sum (x - \bar{x})^2 \sum (y - \bar{y})^2} \right)^2 \quad (5)$$

where n is the count of data points in series; x is the dependent variable and y independent variable; i indicates the associated values of x and y.

Negative bias shows that independent variables sample pool is underestimated against dependant variables sample pool. Dependent variables for hindcasting are the observed data points and for future analysis the base case (modelled hindcast results) data points.

## 2.2.5 Future simulations

For future simulations the RCP4.5 and RCP8.5 scenarios proposed by the IPCC AR5 were considered. The RCP-s (Representative Concentration Pathways) are named according to their radiative forcing target levels for 2100, relative to pre-industrial (1750) levels. RCP4.5 is a rising radiative forcing pathway leading to  $4.5 \text{ W/m}^2$  ( $\sim 650 \text{ ppm CO}_2 \text{ eq}$ ) and stabilizing after 2100. RCP8.5 is a rising radiative forcing pathway leading to  $8.5 \text{ W/m}^2$  ( $\sim 1370 \text{ ppm CO}_2 \text{ eq}$ ) by 2100 (van Vuuren et al., 2011; Meinshausen et al., 2011).

IPCC AR5 relied on the results of Coupled Model Intercomparison Project, Phase 5 (CMIP5). Coupled general circulation models (CGCM) give the basis for assessing climate change, its implications and how the future climate might behave based on chosen concentration pathways. For future simulations the initial conditions were changed by using the data from a single climate model – Model for Interdisciplinary Research on Climate 5 (MIROC5). MIROC5 was a combined effort of Centre for Climate System Research (CCSR), University of Tokyo, National Institute for Environmental Studies (NIES) and Japan Agency for Marine-Earth Science and Technology (Watanabe et al., 2010). MIROC5 uses T85 resolution, which horizontal resolution is  $256 \times 128$  ( $1.40625^\circ \times 1.40625^\circ$ ), which grid cells roughly correspond to about 100 – 150 km across in the mid-latitudes. Number of vertical levels is 40 and grid top is at about 2.9 hPa.

Three variables were extracted from MIROC5 - sea surface temperature (SST), atmospheric air temperature (AAT) and relative humidity (RH). These future variable values were extracted for years 2050 and 2100, where the data for said years were respectively 2045-2055 and 2091-2100 averages for the whole January. The control period (present) variable values were the 2006-2011 average. The future and present variable value differences were calculated with Climate Data Operator. This future-present variable differences are interpolated into WRF metgrid (domain 1-3), which was originally created by WPS (the WRF pre-processing software) using the NCEP FNL data. Thus the obtained differences (as a constant) are added to NCEP FNL data (time-varying) and through that new parameters are set for the WRF model to calculate the future simulations.

Additionally, statistics software R, version 3.2.2, was used in order to assess the standard deviation of wind speed values for the future scenarios (2050RCP45, 2050RCP85, 2100RCP45 and 2100RCP85). For each future scenario the wind speed values were extracted from domain 3 of WRF. Each domain consisted of 89995 coordinate points with 1-hour mean wind speed data. Two time-periods, high wind speed and low wind speed, were chosen to evaluate the deviation in wind speed among different scenarios – 09/01/2005 04:00 UTC when the storm was holding high winds and 10/01/2005 04:00 UTC when the storm had passed and the winds receded.

### **3 Results and Discussion**

#### **3.1 Description of met-ocean conditions during the historic storm Gudrun**

The hurricane known as Gudrun in the Nordic Countries and Erwin in the British Isles and Central Europe crossed the Irish, North and Baltic Sea on 7–9 January 2005. Over the course of the storm, at least 17 people lost their lives in Nordic Countries, including one senior citizen in Pärnu, Estonia. Estimated losses due to wind damage and primarily due to flooding of the urban areas of Pärnu and Haapsalu reached 0.7% of the GDP in Estonia. The previous highest surge (253 cm) took place nearly 38 years earlier and the scale and consequences of the new flooding were quite unexpected both for the population and authorities. The impacts of the storm were most varied (Tõnnisson et al., 2008). Essentially it became the most influential natural disaster for recorded history in Estonia, which received even more media coverage than the Asian tsunami (on December 2004) or the New Orleanian hurricane Katrina (on August 2005) did (Suursaar & Sooäär, 2006). The event activated a broad discussion, as some serious deficiencies in flood forecasting and mitigation abilities in Estonia were revealed.

Gudrun formed as a gradually deepening perturbation of the polar front in the afternoon of 7 January 2005 and moved fast eastward over the British Isles, Scandinavian Peninsula and Finland. Prior to the storm the air temperatures were between –1 and +6°C in Pärnu, while the meteorological norm was around –5°C. It indicated a high energetic status of atmosphere and strong west-flow above the North Atlantic Ocean. The nadir point of 960 hPa was reached northeast of Oslo at 20.00 UTC on 8 January 2005 (Carpenter, 2005). According to the Saffir-Simpson classification, the cyclone reached hurricane strength based upon the maximum mean wind speed measurements both in Denmark and Sweden. According to the Danish Meteorological Institute (DMI), the highest wind speeds reached  $34 \text{ m s}^{-1}$ . Portions of Estonian territory also fell into the zone of the cyclone's strongest wind speeds, which is usually a few hundred kilometres right-hand (i.e. south) from the trajectory of the cyclone centre. Maximum average speeds of SW and W winds went up to  $28 \text{ m s}^{-1}$  on the West Estonian coast and gusts reached  $38 \text{ m s}^{-1}$  (Suursaar et al., 2006). Actual maximum wind speeds could have been even stronger as the malfunctioning measurement equipment due to power outage left gaps in several wind speed records interposed among some very high

readings. Also there were missing or distorted data from some of the tide gauges (Ristna). Therefore many of the storm parameters were later needed to be evaluated with models (Suursaar et al., 2006). The average Baltic Sea level had already been high since December 2004 as a result of the strong cyclonic activity that forced the water from Kattegat through the Danish Straits into the Baltic Sea. As a result of high (+70 cm) background values of the Baltic Sea level, the fast travelling cyclone with a favourable trajectory yielding strong SW-W winds over Estonia, the new highest recorded storm surge occurred in Pärnu, as well as in many other locations along the West Estonian coast (Suursaar & Sooäär, 2006). Sea level height reached 275 cm at 04 UTC, 9 January 2005 according to the Pärnu mareograph data. The densely populated urban areas of Pärnu and Haapsalu were flooded for about 12 hours. New record-high maximum sea levels were also registered at several locations of the Estonian coastal waters. According to sea level hindcast made later, the sea levels in popular resorts like Haapsalu and Kuressaare reached 220 cm (Suursaar et al., 2006). Wave hindcasts indicated that record-high waves (significant wave heights up to 9.5 m) could have been occurred in the Baltic Sea (Soomere et al., 2008).

### **3.2 Hindcast results**

Storm effects to local area are highly influenced by cyclone track and that even more in complex archipelago system such as for the case of Western Estonia. WRF produced base case storm track is shown in Figure 5. The depicted storm track covers 24 hour period from 8 January 12:00 UTC to 9 January 12:00 UTC. Due to the high background air pressure noise it was not possible for Generic Mapping Tool to properly extend the timespan of the cyclone track. The base case simulation results show that WRF was able to reproduce Gudrun's track relatively well, especially during the most crucial time which was around 9 January 00:00 UTC, from where on the storm location was favourable for water build-up at West Estonian coastline, specifically at Pärnu Bay.

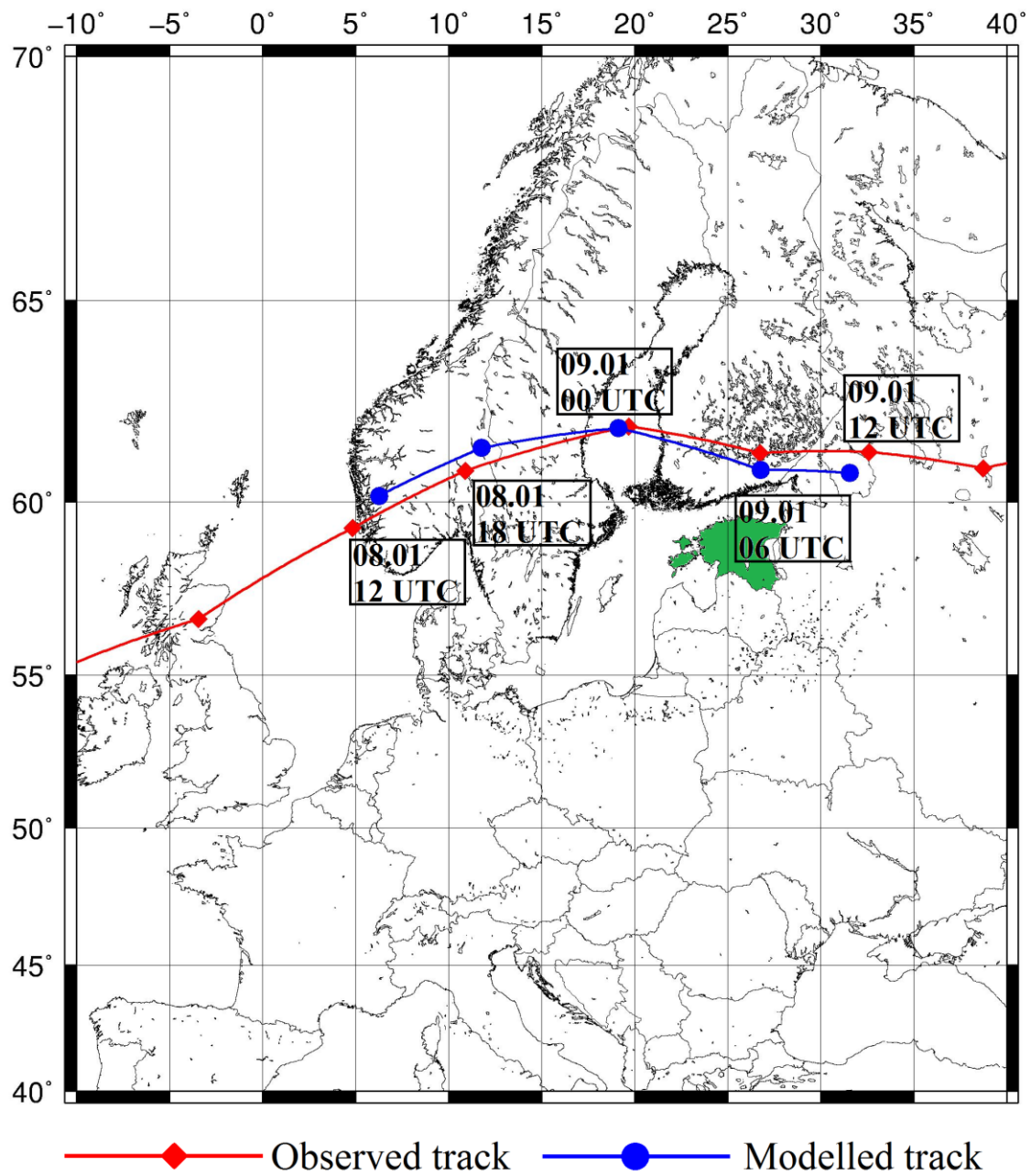


**Figure 5.** Comparison of observed storm track and modelled storm track of Gudrun.

As storm track was well represented by the model, it is then reasonable to assume that the strong wind fields, accompanying the storm to its right side, were also adequately simulated. At the time HIRLAM forecasted and the WRF produced general wind field condition on 9 January 00:00 UTC are presented in Figure 6 – four hours before the observed storm surge maximum. The domain size differences are not ideal for in-depth interpretation of the situation. However, the colour schemes for wind speed follow the same pattern, giving some degree of confidence.

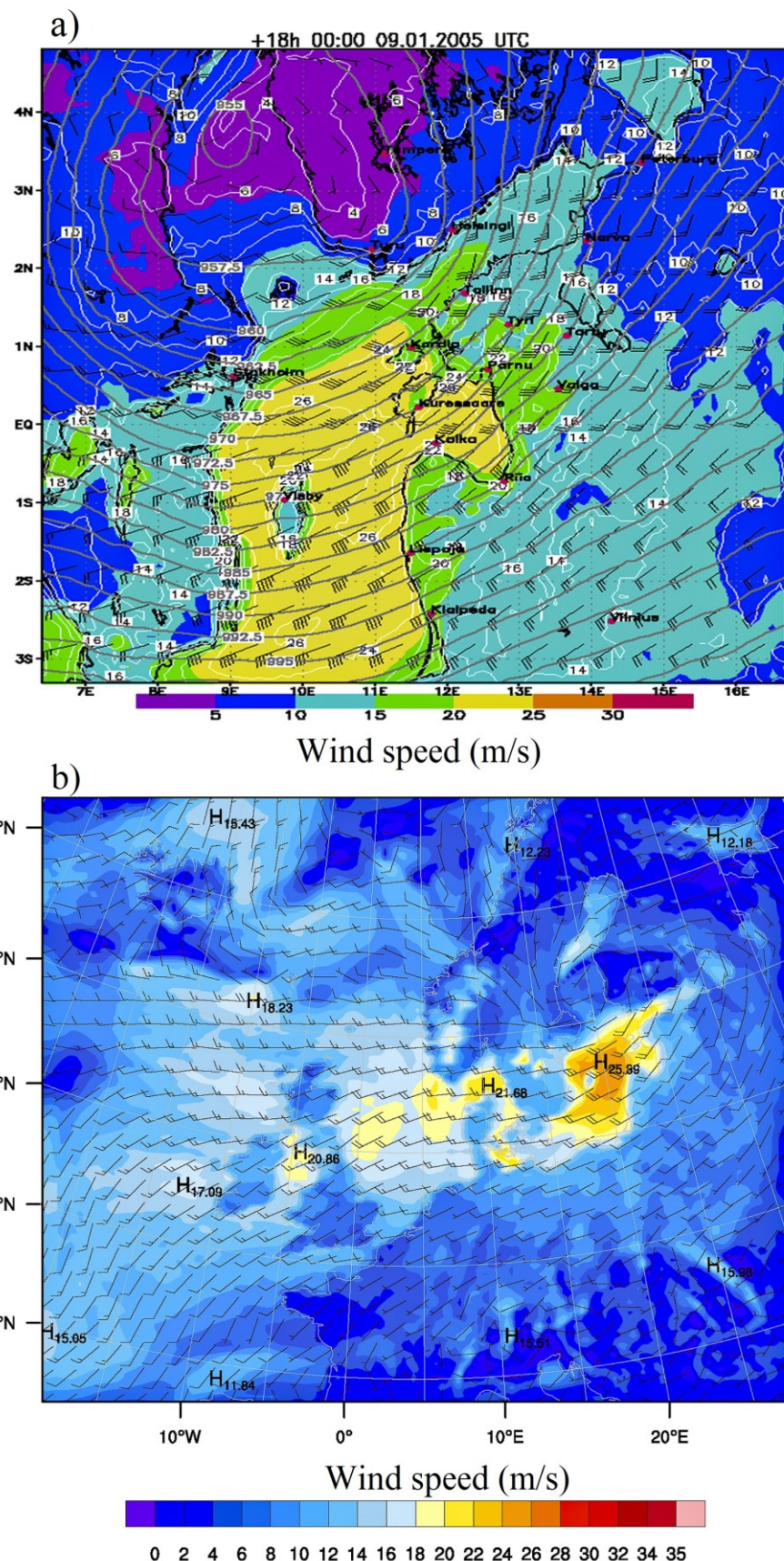


**Figure 6.** Wind field condition on 9 January 2005 at 00:00 UTC a) HIRLAM forecast results at the time of the event ([www.emhi.ee](http://www.emhi.ee) website); b) WRF produced results over domain 1.

Drawing correlations based only on visual observation over vast areas does not yield in objective results, it is therefore necessary to investigate storm parameters in more detail. The simulation results for wind speed and direction were backtested against observation data from seven meteorological stations. Interestingly, some of the observed results however might not be strictly more accurate than the simulated results. This is due to aforementioned technical failures. In addition, meteorological stations are sheltered to a various extent from different sectors and thus having inherently certain degree of uncertainty in measured wind speed and direction values (see Figure 1). Nonetheless, the simulation results were mostly in a good agreement with the observations (Figure 7). Furthermore, the statistics analysis for wind speed and direction in Table 2 gives a more comprehensive interpretation for these results.

Sõrve station had the least data points due to the operational failures during the storm and with that forethought in mind it is not covered in more detailed analysis, however is shown in relevant figures and tables. In terms of wind speed, the best concurrence was found for the case of Pärnu-Sauga, showing slight negative bias. Good results were also seen for Ruhnu and Kihnu stations, which in fact hold higher priority in terms of representing and evaluating the cause-and-effect of storm surge build-up at Pärnu. Reason being, that these stations are well situated in the Gulf of Riga and more accurate simulations over the said water body also yield better results for storm surge simulations. As opposed to wind speed, the wind direction in Ruhnu was statistically the least favourable and this can be attributed to the local sheltering objects nearby the anemometer mast. But on the other hand the dominant modelled wind direction, prior to peak wind speeds, was from sectors 210-230 degrees, on the contrary to observed 210-250, which in return would indicate to a more favourable conditions for storm surge build-up at Pärnu (Figure 8). Kihnu station on the other hand displayed the best results for wind direction.

Accurate hindcasts are crucial for models verification, however some discrepancies were also found in the simulation results. The largest overall disagreements between observations and simulations was for the case of Vilsandi station (see Appendix 1&2), where the winds from the 210-250 sector are underestimated due to the close proximity of the lighthouse and buildings (Jaagus & Kull, 2011). These artificial constructions cause an explicit effect for capturing accurate wind speed measurements. As seen for wind speed scatter plot in Figure 7, the observed and modelled data points coincide with relatively high accuracy before and after the wind direction shifts from the “shadow sector”. Additionally, Ristna and Virtsu station also exhibited poor results.

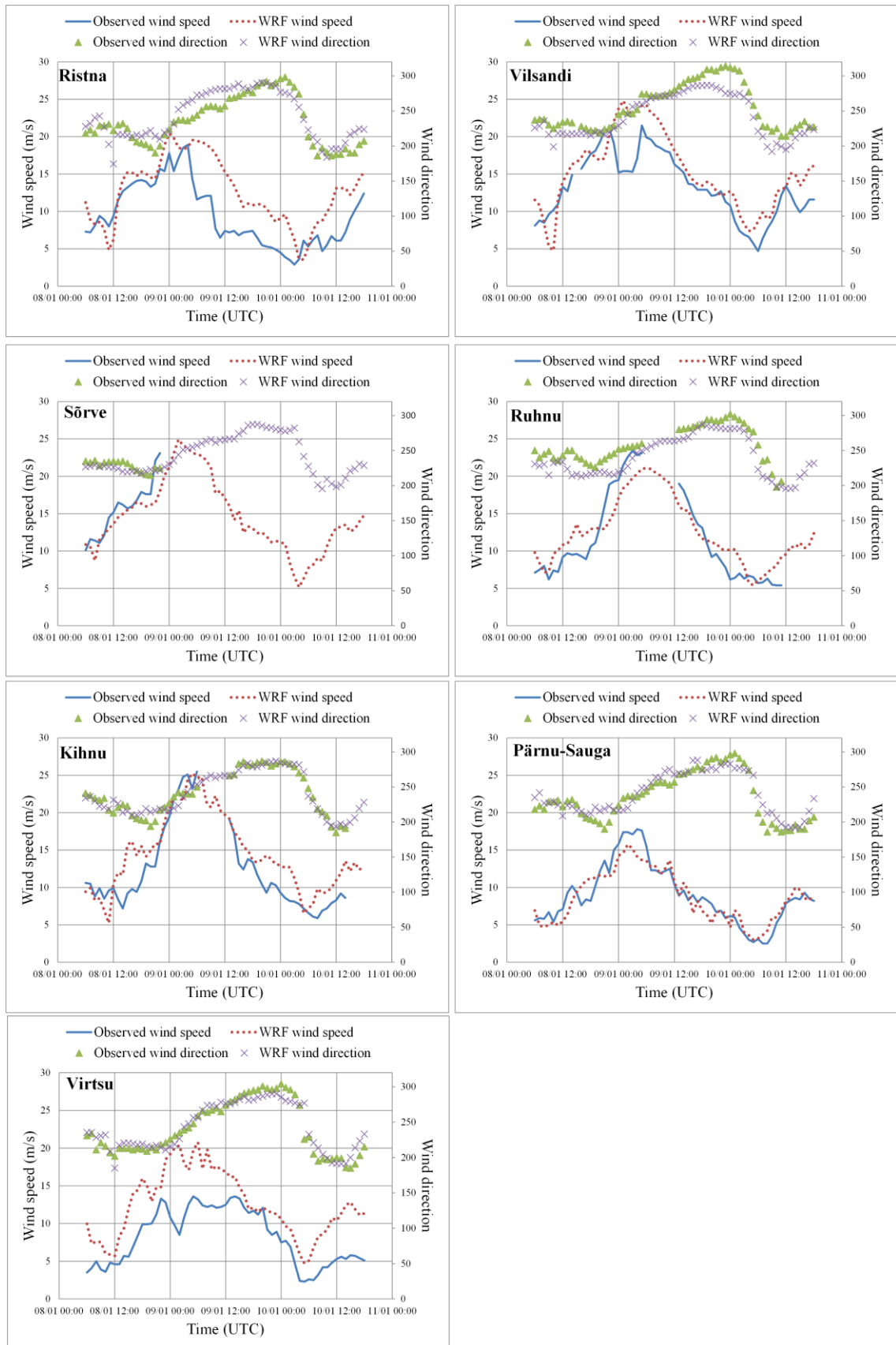


**Figure 7.** Wind speed and direction hindcast results for 7 weather stations (see Figures 1&4 for locations).

Likewise to Vilsandi, their measurement accuracy is inhibited by local natural and artificial obstacles around meteorological field, thus failing to provide adequate wind data which would explain the true characteristics of wind parameters. Furthermore, the differences might arise due to the relatively low horizontal topography resolution of the WRF which in return makes it more difficult to extract the calculation values with high precision. Also, the gridded model winds are usually quite smooth and cannot take into account small-scale local features, especially on the land-sea interface.

**Table 2.** Hindcast statistics results for wind speed, direction and sea level. Negative bias shows that the simulated variable values were underestimated against observations.

Weather station	Wind speed (m/s)		
	RMSE	Bias	R <sup>2</sup>
Ristna	4.31	3.02	0.58
Vilsandi	3.81	1.96	0.72
Sõrve	2.24	-1.45	0.80
Ruhnu	2.46	0.34	0.87
Kihnu	2.92	1.76	0.81
Pärnu-Sauga	1.61	-0.28	0.84
Virtsu	4.70	3.93	0.69
<hr/>			
Wind direction			
<hr/>			
Ristna	17.37	6.54	0.79
Vilsandi	32.62	-9.94	0.90
Sõrve	7.50	-5.08	0.36
Ruhnu	19.14	-16.68	0.89
Kihnu	8.51	-0.11	0.93
Pärnu-Sauga	13.42	4.10	0.87
Virtsu	12.29	1.53	0.90
<hr/>			
Sea level (m)			
<hr/>			
Pärnu tide gauge	0.13	0.28	0.89

The simulation results for the 2005 Gudrun show that during the peak moments of the storm the sea water was pushed to the shallow enclosed  $411 \text{ km}^2$  Pärnu Bay, causing the funneling effect where the water inflow exceeds the outflow. The simulated storm surge height at the mouth of the Pärnu river shows good agreement with observations, where the first peak maximum difference was just 2.2% or, 6 cm (Figures 9&10). This further increases the confidence that the modelled wind field was reasonably well simulated (Figure 6). FVCOM was able to reproduce two surge height peaks where the occurrence of the second peaks lies not on the wind field but rather on the oceanography of the Gulf of Riga. The formation of the second peak is likely due to the 5-hour seiche (self-oscillation) period of the Gulf of Riga basin (Suursaar et al., 2003). However it was slightly overestimated by the model.

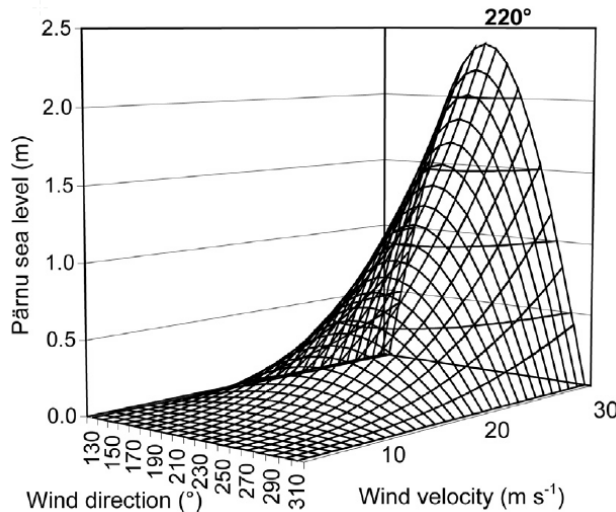


**Figure 8.** Modelled Pärnu sea level in dependence from wind speed and direction, blowing uniformly over the Gulf of Riga (after Suursaar et al., 2003).

The biggest notable difference is the extended period of the storm surge event (Figure 10) where the simulated water levels did not drop as fast as it was observed. It also explains the positive bias (see Appendix 3). This however can be related to the similarly prolonged wind effect during the storm and to the higher aforementioned smoothness of the model (Figure 7). Furthermore, there is an increase in simulated surge height before the first peak, starting after 8 January 12:00 UTC. This however might be explained by observing the simulation results for Kihnu and Ruhnu (Figure 7) where at that time WRF produced stronger winds as were observed. Stronger simulated winds blowing from sectors 215-230 can be one of the causes in producing greater initial surge height at Pärnu (Figure 8).

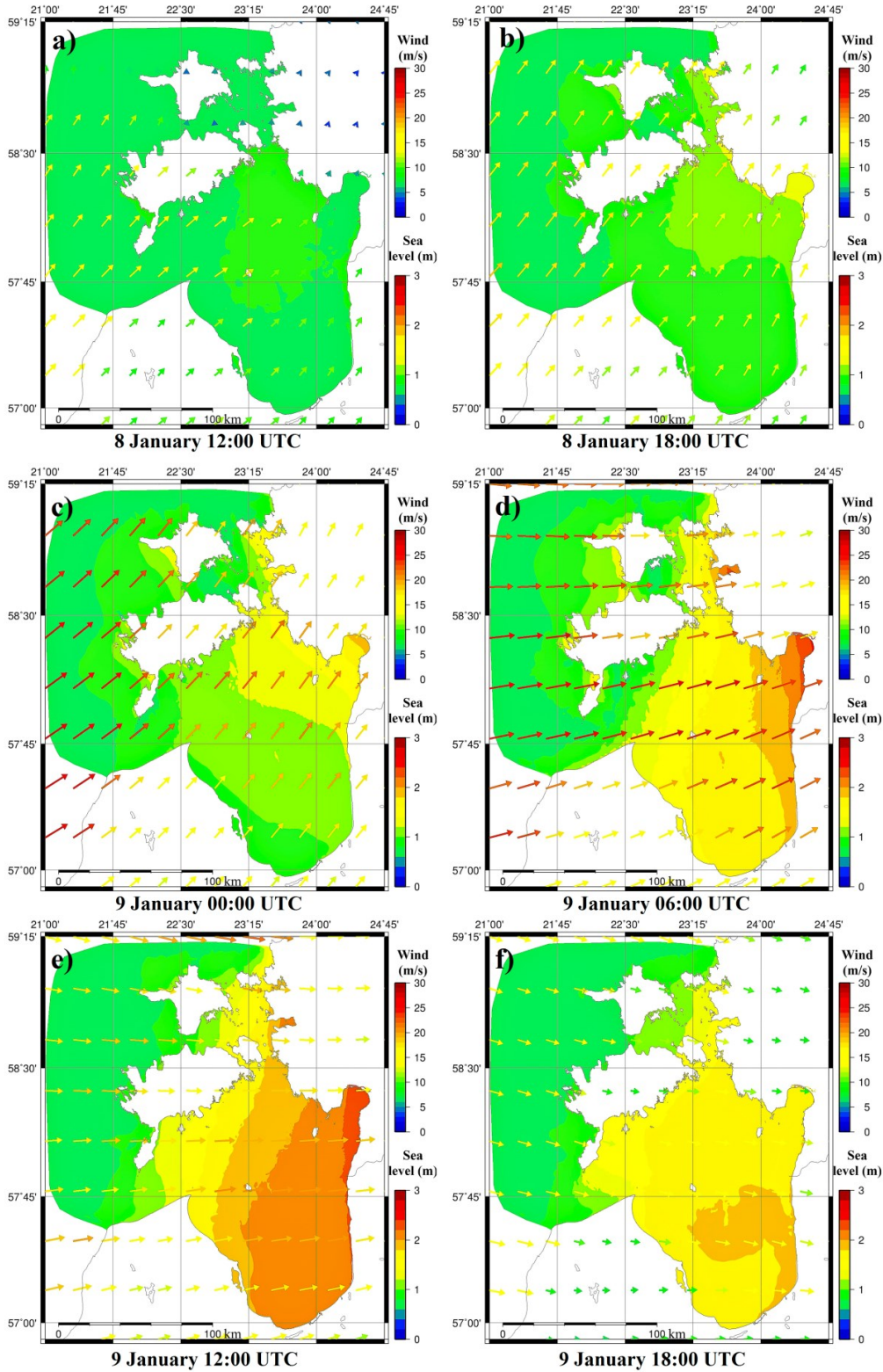


**Figure 9.** Spatial sea level patterns for base case simulation showing the wind speed and direction results with 6-hourly time-step.

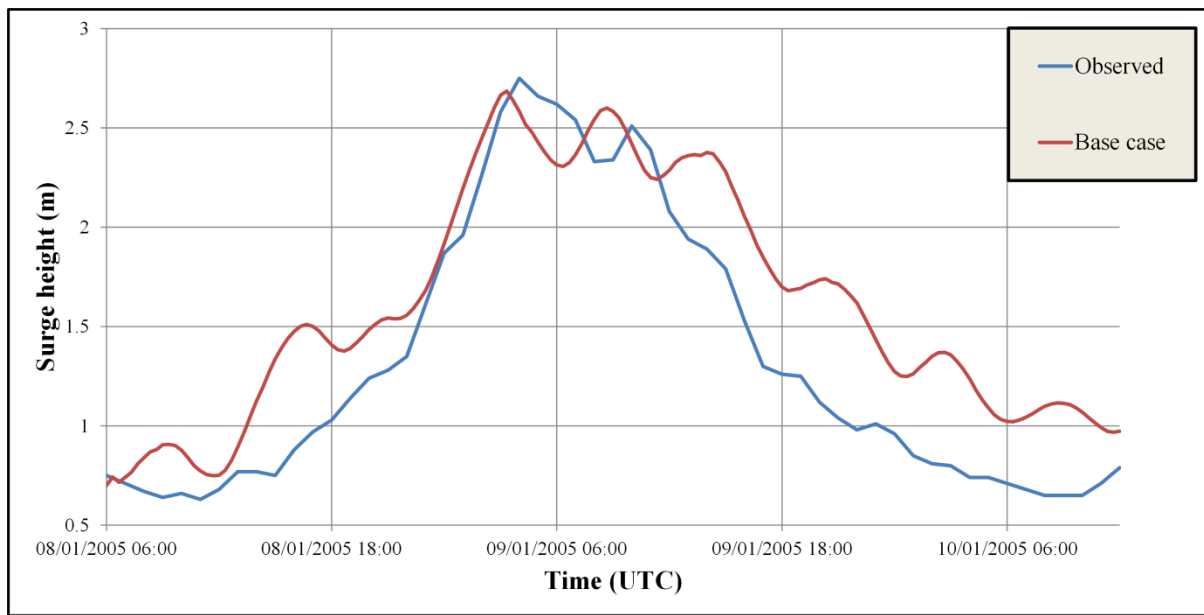


**Figure 10.** Observed and modelled storm surge height at the Pärnu tide gauge.

### 3.3 Projections of extratropical-cyclones according to Global Climate Models

How climate change under CMIP5 global warming projections affects the behaviour of ETC-s has captured interests of many studies, with focus being shifted to multi-model ensembles. It is apparent that a great number of research aim their attention at the response of storm tracks (Ulbrich et al., 2008, Chang et al., 2012, Harvey et al., 2012, Zappa et al., 2013), which seem to show a more poleward shift. Similar results were drawn by Woolings et al. (2012) while using CMIP3 models, relating to the extension and intensification of eddy driven jet towards western Europe. On the other hand, Mizuta (2012) found in a number of models an enhanced polar jet over North Pacific, but less agreement was found for over the North Atlantic. According to a literature review conducted by Bader et al. (2011) the most agreed upon result is that observations and future projections of the mid-latitude storms are exhibiting a poleward shift. However in terms of intensity, uncertainty remains. Moreover, the IPCC AR5 goes into great detail over research and findings for future climate change and ETC-s response to these changes in a warmer climate. It concludes that most studies agree upon a more poleward shift of ETC-s trajectory in Southern Hemisphere and with lesser certainty that the same extent in shift applies in the Northern Hemisphere (Christensen et al., 2013).

As for the Baltic Sea region and Estonia in particular, little research is found on future ETC-s. Studies on historical climate variability in the Baltic Sea and Estonia show an increase in

westerlies during the second half of 20<sup>th</sup> century (Jaagus, 2006; Lehnmann et al., 2011). Feser et al. (2015) conducted a comprehensive review of storminess over North Atlantic and Northwestern Europe. Their findings indicate that for the Baltic Sea there is a larger variance in studies for the past storm trends, highly depending on the data and time periods used. Studies on future projections for the Baltic Sea and central Europe show the same number of increasing and decreasing trends. In terms of extreme wind events, Knippertz et al. (2000) called attention to climate models resolution, which need to improve in order to better represent orography, the land-sea distribution and etc. Recent study about CMIP5 models capability to capture the observed behaviours of North Atlantic ETC-s by Zappa et al. (2013) suggests that high resolution (about T106 or N96) might be necessary for a good simulation of North Atlantic storm tracks in the boreal winter months, whereas for boreal summer months the lower resolutions might already be sufficient.

### **3.4 Characteristics of storm Gudrun under future climate change scenarios**

Climate change induced global warming scenarios RCP4.5 and RCP8.5 were investigated for the case of historical storm Gudrun projected into the years 2050 and 2100. The initial conditions were modified by extracting and forcing three parameters (SST, AAT, RH) to the atmospheric model WRF-ARW. The obtained change in MIROC5 parameter values are relative to the reference area (domain 1) average for January 2006 – 2011. The changes in SST under applied conditions are 0.25, 1.16, 1.22 and 2.80 K for 2050RCP4.5, 2100RCP4.5, 2050RCP8.5 and 2100RCP8.5, respectively.

The change in AAT and RH values as area averages are shown on Figures 11&12. The vertical air pressure gradient starts from 1000 hPa and ends at 10 hPa representing the pressure levels at sea level and at around 32 km altitude, respectively. The most notable difference is perhaps that under simulated future conditions the AAT change in 2050RCP8.5 is the least significant while the SST it is the second highest. In fact the SST for 2100RCP8.5 is more than twice that of the second highest, 2050RCP8.5, value.

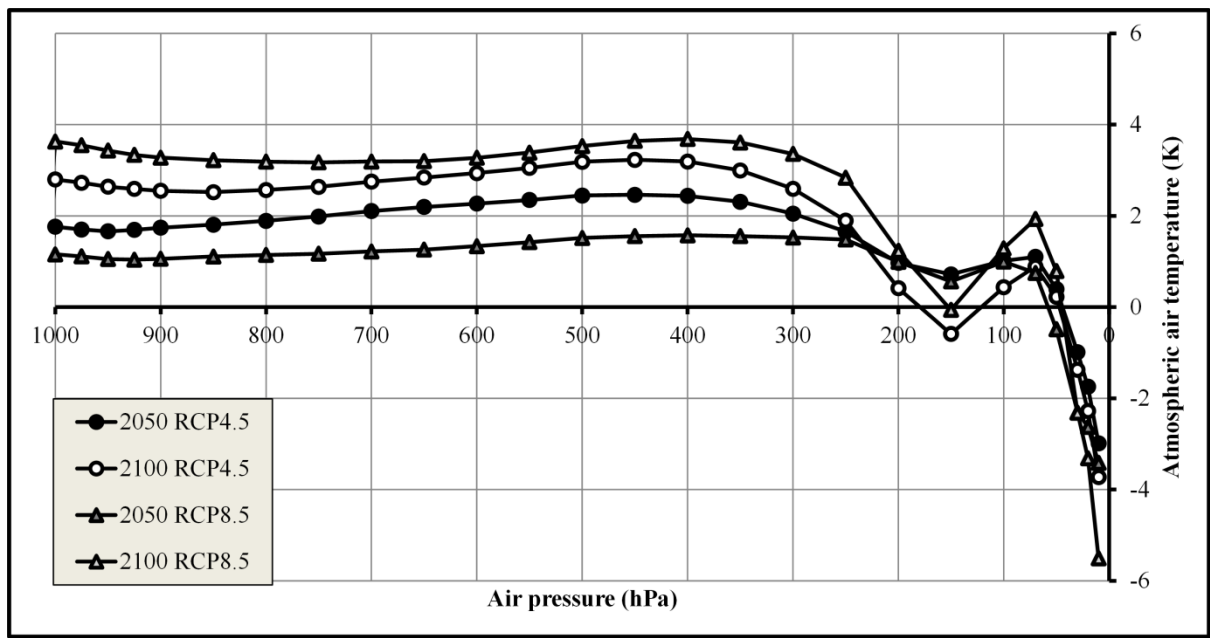


**Figure 11.** Change in atmospheric air temperature under future scenarios. Height increases from left to right ( $100 \text{ hPa} \approx 16 \text{ km}$ ).

As for the case of SST and AAT, the RH also shows an increase during the observed period of up to 200 hPa, which at mid-latitudes is roughly somewhere between troposphere and stratosphere. According to a study conducted by Booth et al. (2013), the increase in moisture will not lead to a stronger magnitude of extreme storms at mid-latitudes. However it might increase storm growth rates and the number of moderate storms.

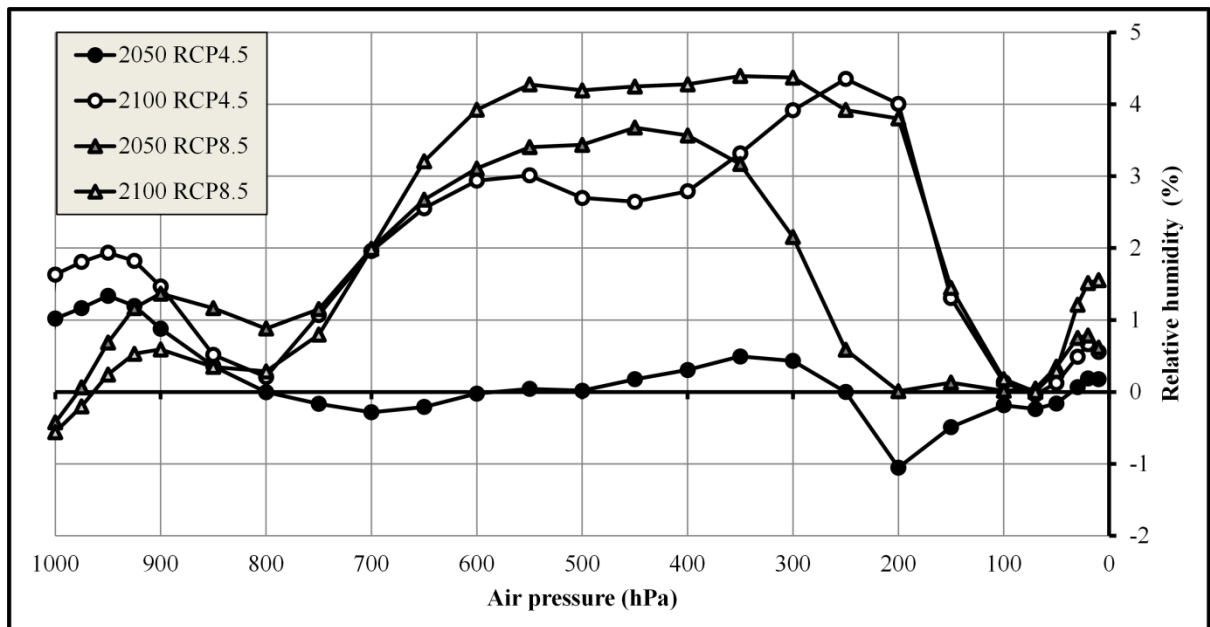


**Figure 12.** Change in relative humidity under future scenarios.

As previously mentioned, the storm tracks can influence the storm effects with a specific location in mind. Because of that it is necessary to distinguish if for the future simulations there were any shifts in storm tracks that might alter the effects. All the future cases except for one showed good fit with the observations and, especially for reference purposes, with modelled track (Figure 13).

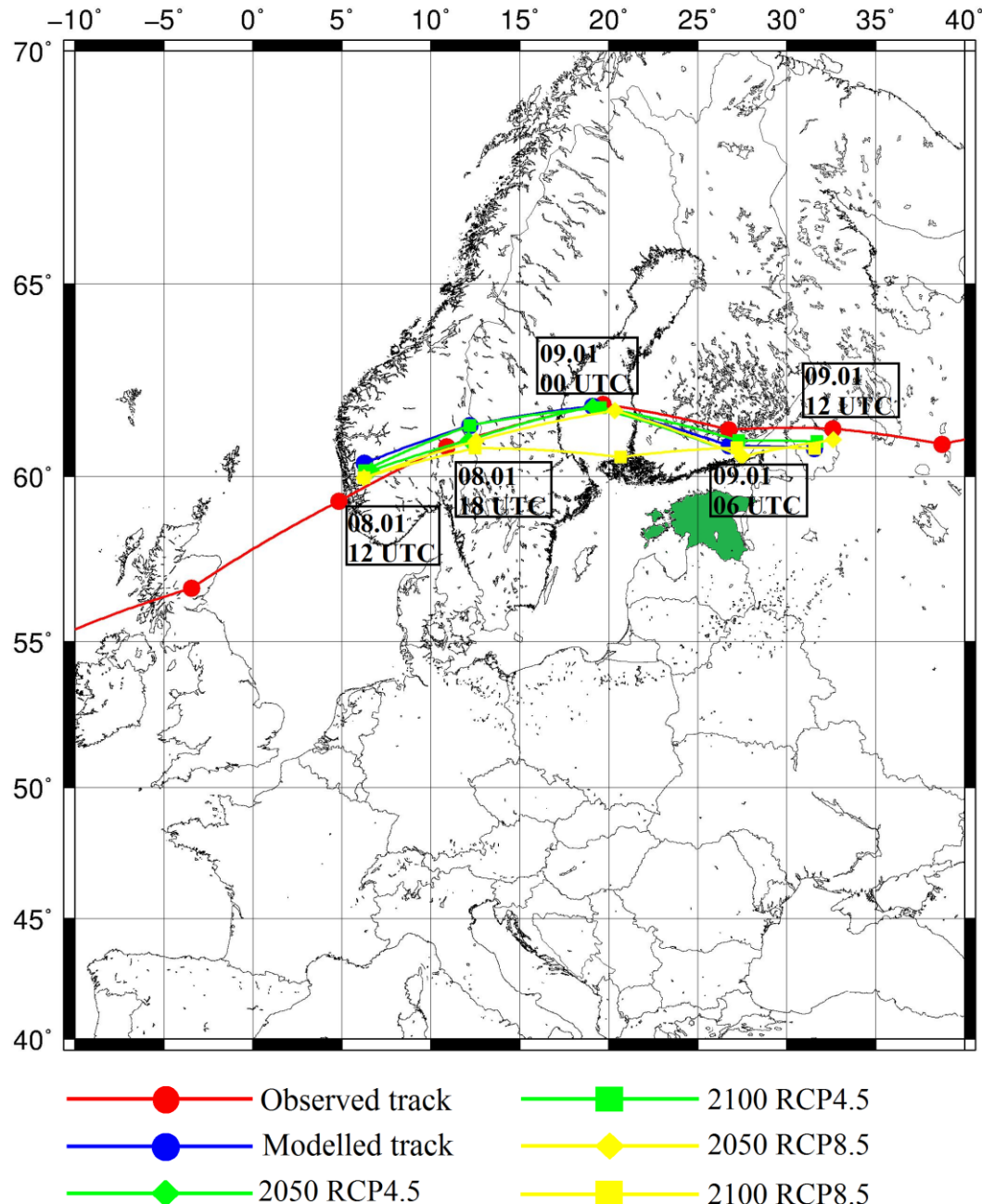


**Figure 13.** Storm track comparison between observation, modelled and future scenarios. Location of Estonia is marked as dark green.

The odd one out was the future scenario 2100 RCP8.5, exhibiting a southward shift. However, closer analysis of that particular storm track showed that during 9 January 00:00 UTC the sea level pressure of the strongest forcing scenario showed rather wide area of nearly equal, low values. The sea level pressure difference in its current MSLP track and that of the location of others was few decimal places. But the GMT software picks out the absolute minimum. For that reason it is assumed that the storm track of 2100 RCP8.5 still matches that of the other scenarios and has no remarkable change on the simulation results at locations of interest.

### 3.4.1 Wind speed

In order to evaluate future storm surges under changed climate conditions it is necessary to determine whether there was change in wind speed and direction, which may or may not cause differences in the surge height at Pärnu. For future cases, four weather stations, Vilsandi, Sõrve, Kihnu, Ruhnu, were chosen to compare against the base case results (Table 3). The criterion for station selection was to get an assessment for wind parameter conditions over the Gulf of Riga. For this case, on the contrary to hindcasting, Sõrve station was also included due to its location at the southern tip of Saaremaa, thus giving a good representation of winds coming from the Baltic Proper. Furthermore, the hindcasting results showed good results and the disagreements were mostly due to the local natural and artificial obstructions, thus giving reason to assume that the base case calculation is suitable for comparison with the future calculations at Sõrve station.

Statistics show that two stations, Vilsandi and Kihnu, had the tendency to underestimate the wind speed with the exception of 2100 RCP8.5 at Kihnu, which showed insignificant overestimation (see Appendix 4). Also these two stations had the smallest change in terms of RMSE, especially for both RCP8.5 cases. The largest RMSE, for both, were under 2100 RCP4.5 scenarios. Sõrve and Ruhnu station, forming the central part of the selected stations (Figure 4), on the other hand showed the tendency to be overestimated. Moreover, they showed higher values of RMSE, indicating increase in wind speeds. Most considerable change in wind speed among selected stations were for the 2050 RCP8.5 and 2100 RCP8.5 scenarios at Ruhnu and Sõrve, respectively.

### 3.4.2 Wind direction

Without any exception all the selected stations showed tendency to underestimate the wind direction. Among all the scenarios the closest results with the base case was for the 2050 RCP8.5 and closest to perfect fit was observed for Sõrve station (see Appendix 5). The largest differences occurred at Vilsandi and Kihnu station, especially between the key sectors of 210-230 degrees. These differences are mostly due to underestimation of wind direction, however there is no clear pattern.

**Table 3.** Future scenarios wind speed and direction statistics results. Negative bias shows that the simulated variable values were underestimated against observations.

Weather station	Wind speed (m/s)				Wind direction				RMSE
	2050 RCP4.5	2050 RCP8.5	2100 RCP4.5	2100 RCP8.5	2050 RCP4.5	2050 RCP8.5	2100 RCP4.5	2100 RCP8.5	
Vilsandi	1.30	1.09	1.43	1.26	7.64	4.86	7.69	6.49	
Sõrve	1.60	1.62	1.87	2.00	4.82	2.26	4.92	4.50	
Ruhnu	2.09	2.30	2.16	2.24	7.67	2.56	7.46	5.66	
Kihnu	1.63	1.11	1.66	1.25	7.49	4.43	7.18	7.56	
<hr/>									
Vilsandi	-0.56	-0.05	-0.57	-0.22	-1.28	-1.01	-1.14	-2.00	
Sõrve	1.27	1.47	1.24	1.25	-2.15	-0.64	-2.16	-1.81	
Ruhnu	1.66	2.18	1.74	2.07	-1.32	-0.72	-1.43	-1.63	Bias
Kihnu	-0.64	-0.01	-0.61	0.02	-1.44	-0.43	-0.94	-1.61	
<hr/>									
Vilsandi	0.95	0.96	0.93	0.94	0.94	0.98	0.94	0.96	
Sõrve	0.96	0.98	0.93	0.90	0.98	0.99	0.97	0.98	
Ruhnu	0.94	0.99	0.94	0.97	0.93	0.99	0.93	0.97	
Kihnu	0.91	0.95	0.91	0.94	0.94	0.98	0.95	0.94	R <sup>2</sup>
<hr/>									

All things considered there does not seem to be any significant changes in wind speed or direction that might cause any substantial change in the storm surge height at Pärnu. Rather there are slight shifts in under- and overestimations which all in all cancel each other out or change so little that they lack the potential to induce any significant surge growth.

### 3.4.3 Surge height

FVCOM was adequately able to reproduce the Gudrun induced surge height at the Pärnu tide gauge. However under the changed climate conditions there was no increase in maximum surge height compared with the base case results (Figure 14). Furthermore, the RMSE shows very little change (Table 4) leading to conclusion that, considering the change in SST, AAT and RH, there is no significant change in storm surge height under used parameters. In fact a slight decrease was observed for all the future scenarios (see Appendix 6). The first peak maximums are 2.65, 2.62, 2.59 and 2.58 m for 2100 RCP4.5, 2050 RCP4.5, 2100 RCP 8.5 and 2050 RCP8.5, respectively. RCP4.5 scenarios, compared to RCP8.5, showed bigger surge heights, however not by much. They also exhibited a larger local minimum between the two maximums. Another notable change is that RCP8.5 cases showed more stable decline in surge height than other cases.

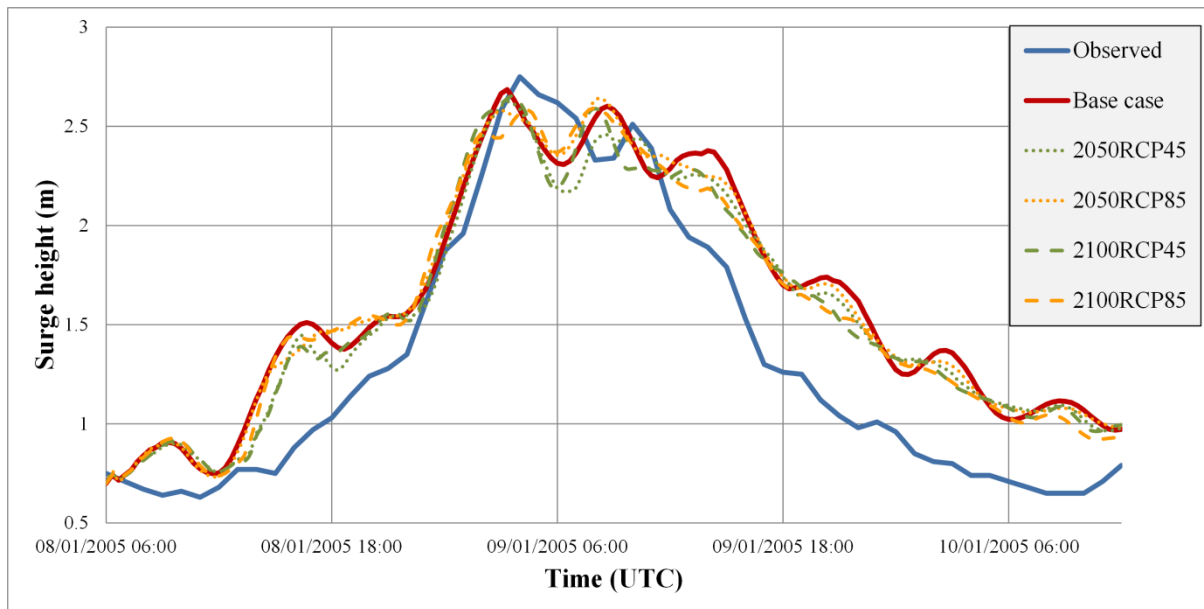


**Figure 14.** Storm surge height comparison between observations, base case and all the future scenarios at Pärnu tide gauge.

However considering all the established facts, it is feasible to assume that such little differences might have occurred due to previously assessed wind fields, which showed some minor variations – not enough to make a considerable difference but enough to cause slight changes. Additionally it does not necessarily mean that some other locations experienced the same outcome. Since the surge height potential at Pärnu is highly sensitive to wind direction it could be that locations which are more open to wider range of wind effects, could have received slightly stronger surges.

**Table 4.** Storm surge height statistics results for future scenarios at Pärnu tide gauge.

Scenario	Storm surge height (m)		
	RMSE	Bias	R <sup>2</sup>
2050 RCP4.5	0.08	0.05	0.99
2050 RCP8.5	0.05	0.00	0.99
2100 RCP4.5	0.09	0.04	0.98
2100 RCP8.5	0.09	0.03	0.98

### 3.4.4 Standard deviation of wind speed

Further analysis of wind speeds under future scenarios using standard deviation is shown in Figure 15. The main aim of this analysis was to better understand how WRF generated higher and lower wind speeds under future conditions. The standard deviation considers only future scenarios. At a brief look it becomes evident that there are considerable variations in lower and higher wind speeds. The standard deviation is much smaller at high wind speeds (Figure 15a). Towards further south from the storm track, the smaller the deviations become. This is particularly clear for the majority of Gulf of Riga, Irbe Strait and Baltic Proper under the 58° latitude. The larger deviations seems to be present at “wind gusts” moving counterclockwise from the eye of the storm and increasing the further closer to the storm they are and also on larger waterbeds.

Lower wind speed conditions are different from that of the high speed (Figure 15b). In these conditions two distinct patterns evolve. Firstly, the standard deviation is smaller over land areas where it seems that the wind speeds become more balanced due to the roughness of surface topography. Secondly, large differences occur over waters, which is probably because under lower wind speed the water surface induced drag can have higher effect on the wind velocity. However it is highly unlikely that these deviations are due to model run particularities. Future wind speed forecasts showed very little change over the simulation period, including both high and low wind speeds. Figure 15 on the other hand focuses on the specific hourly averaged standard deviation of highs and lows of future scenarios. Indicating that higher wind speeds have larger likeness among the future scenarios and lower wind speeds have less.

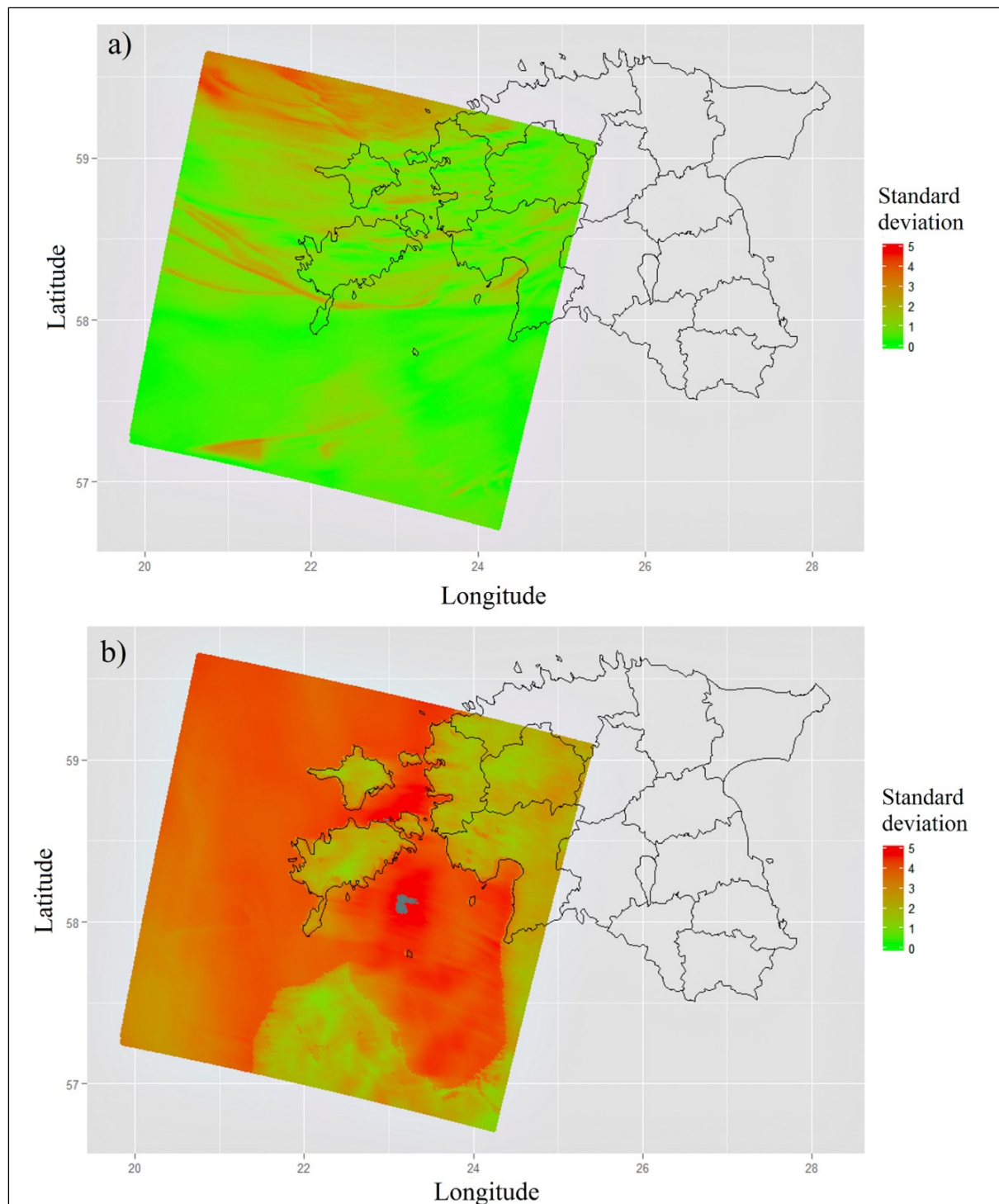


**Figure 15.** Standard deviation (m/s) map of future scenario wind speed results where a) is wind speed in future corresponding to Jan. 9, 2005 conditions at 04:00 UTC and b) is wind speed in future corresponding to Jan. 10, 2005 conditions at 04:00 UTC. Grey spot indicates that the deviation exceeded 5 m/s limit.

High winds (from favourable direction) are the main cause for significant surge build-up and it is evident that these highs had very little or no deviation among the future scenarios under the 58<sup>0</sup> latitude. The lack of change in extreme winds gives further insight to why among the future scenarios there was no increase in storm surge height at Pärnu. However in some other locations (open areas due north from 58<sup>0</sup> latitude) there might have been higher surges compared to observations, though they were not investigated in the current study.

### **3.5 Final remarks and proposals for further research**

The results of present study indicate that under applied conditions and methodology, the future ETC-s might not intensify as opposed to general belief. This however is probably due to the mechanisms of ETC-s, which accumulate their energy from temperature gradient at the polar front. As a result, under warmer climatic conditions that might hinder the intensification of such storm systems. Interestingly, studies applying the same methodology for tropical cyclones (Tasnim et al., 2015; Nakamura et al., 2015b, 2016) have shown intensification of future storms. These tropical low pressure systems derive their energy from warm water evaporation. This demonstrates that the models can adequately simulate different types of storm systems.

The methodology does not include however large scale changes in geophysical fluid dynamics, such as water cycle, snow, ice etc. For instance a study conducted by Hansen et al. (2016) indicates that if the ice sheets over Greenland will melt, then it might cause a major change in the North-Atlantic oceans circulation which in return might lead to stronger ETC-s (superstorms). For that reason it is necessary to further investigate possible future scenarios by studying projections, establishing new methods and improving existing ones.

With that forethought in mind the author of this study proposes improvements for future research. In order to achieve more substantial results on how the future ETC-s might affect Estonia, and its coastal settlements in particular, the following factors should be taken under consideration:

- 1) ratio between post-glacial rebound and sea level rise;
- 2) extend high topography and bathymetry data coverage in the FVCOM model;
- 3) include river discharge (eg in Pärnu) because the ETC-s in the future have the potential to carry more moisture polewards;
- 4) use high resolution atmospheric reanalysis data (ERA-Interim);
- 5) Broaden domain 1 size and increase simulation run time;
- 6) apply ensemble approach including a number of CMIP5 global climate models;
- 7) simulating various storms (with changing tracks) over different seasons

## 4 Conclusions

Extra-tropical cyclones are considered to be the most dangerous natural hazards in the Baltic Sea region, causing strong winds, floods and heavy rain. During the 21<sup>st</sup> century there has already been a number of devastating storm events in the world. It is necessary for coastal communities to address the dangers associated with such events and understand how they might behave in the future climate. In Estonia, the most notable recorded storm is considered to be the 2005 January storm Gudrun. High wind speed and favourable dominant wind direction during peak hours caused record high flooding's in a number of coastal communities, including +275 cm at Pärnu City. The study at hand aims to find out how Gudrun would behave under future climate conditions.

The study applied well known atmospheric model (ARW-WRF) and ocean model (FVCOM) to simulate the past and future Gudrun. The WRF model was run with NCEP FNL Operational Global Analysis data and the results were compared against observed observational data from selected meteorological stations to confirm the models capability in simulating the past event. Two scenarios, RCP4.5 and RCP8.5, were selected for future simulations for years 2050 and 2100 as possible pathways. Three parameters (sea surface temperature, atmospheric air temperature and relative humidity) were chosen from these scenarios, which were acquired from MIROC5 global climate model projections. These parameter differences were then interpolated to past Gudrun's meteorological grids.

The modelled wind speed and directions, for the most part, were in good agreement with the observations, where the noticeable differences only occurred due to artificial obstructions. Among the meteorological stations the best concurrences were found to be for Kihnu and Ruhnu stations, thus well representing the wind conditions over the Gulf of Riga. Storm surge simulation near the Pärnu tide gauge was also produced with high accuracy, where the first peak difference was just 2.2 % (6 cm). The applied models were successfully validated for this specific case study, therefore giving reason to proceed with future simulations.

Scenarios 2050RCP4.5, 2100RCP4.5, 2050RCP8.5 and 2100RCP8.5 were considered for future simulations. The most extreme RCP8.5 scenarios show highest (up to 2.8 K) changes in SST over the control period. The scenarios also show rise in AAT up to 50 hPa. In terms of RH, an overall increase is found for the better part of stratosphere (up to 200 hPa), with the exception of 2050RCP4.5. Considering all of these changes in meteorological forcings, the models did not yield in a higher surge height at Pärnu. Closest surge heights to base case

(hindcast) among the future scenarios were for the 2100 and 2050 RCP4.5, respectively. Among scenarios there were some slight changes to wind speed and direction, when compared against the base case. These minor variations might have also been the probable cause for slight changes in surge heights at Pärnu. Also standard deviation analysis showed that higher wind speeds among future scenarios have much smaller deviations under the 58<sup>0</sup> latitude, whereas the lower wind speeds show larger deviations. This suggests that among future scenarios there were no big changes in wind speed that might cause higher surge build-up at Pärnu.

This study focused on one particular storm case. However no strong generalizations can be made from an individual storm study. In order to reduce uncertainty, it is necessary to further develop the methodology at hand. Also more simulations for different seasonal storms and tracks must be conducted to attain more concrete results on how future extra-tropical cyclones might behave under changing climate conditions.

# **Tulevikutormide simuleerimine, kasutades atmosfääri- (WRF) ja ookeanimudelit (FVCOM) 2005. aasta jaanuaritormi (Gudrun) näitel**

**Martin Mäll**

## **KOKKUVÕTE**

Läänemere regioonis kujutavad klimaatilistest teguritest suurimat ohtu parasvöötme tsüklonid, millega kaasnevad tugevad tuuled ja sademed, mis võivad põhjustada tormikahjustusi ja üleujutusi. Viimastel aastakümnetel on esinenud mitmeid katastroofiliste tagajärgedega torme. Sellest tulenevalt on oluline parendada rannikulinnade valmisolekut ja mõista kuidas tormid muutuvad tuleviku kliimas. Suurima mõjuga parasvöötme torm Eestis oli 2005. a jaanuaritorm Gudrun, mis põhjustas rannikulinnades rekordtasemel üleujutusi. Pärnu linna mareograaf mõõtis veetaseme tõusuks +275 cm üle nulli. Käesoleva uurimustöö eesmärk on uurida, milline oleks Gudruni laadne äärmuslik torm tuleviku kliimatingimustes.

Simuleerimaks mineviku ja tuleviku Gudrunit kasutati atmosfäärimudelit ARW-WRF ja ookeanimudelit FVCOM. Järelarvutuse sisendandmed WRF-i käitamiseks saadi NCEP FNL operatiivanalüüsist. Järelarvutuse tulemuste võrdluseks kasutati Eesti Keskkonnaagentuurilt saadud tunnise intervalliga tuule kiiruse, suuna ja veetaseme vaatlusandmeid valitud rannalähedastest jaamadest. Tulevikustsenariumide saamiseks asendati algsed NCEP järelarvutuse merepinna veetemperatuuri, õhutemperatuuri ja suhtelise õhuniiskuse andmed MIROC5 mudeli abil saadud tuleviku jaoks manipuleeritud andmetega. Selles töös arvestati IPCC AR5 raportis toodud RCP4.5 ja RCP8.5 stsenaariumidel põhinevaid kliimaprojektsioone aastatele 2050 ja 2100. Nii järelarvutuse kui ka tuleviku arvutuste tulemusi analüüsiti statistiliselt.

Simuleeritud tuule kiirus ja suund olid vaatlusandmetega ligilähedases korrelatsioonis, kuid teatud erinevused tulenesid vaatlusjaamade läheduses asuvatest hoonetest. Järelarvutuste seas oli kõige parem kokkulangevus Kihlus ja Ruhnus, mis kinnitab, et Liivi lahel simuleeritud tuuletingimused olid heas vastavuses mõõdetud vaatlusandmetega. Veetaseme järelarvutus Pärnu jõe suudmes oli samuti heas vastavuses vaatlusandmetega, kus tormitõusu esimese tipu kõrguse erinevus oli vaid 6 cm. Realistikud järelarvutuse tulemused olid eelduseks tuleviku simulatsioonide arvutamiseks.

Ekstreemseim tuleviku stsenaarium RCP8.5 näitas kontrollperioodi suhtes suurimat merepinna temperatuuri tõusu (kuni 2.8 K). Kõik stsenaariumid näitavad ka atmosfääARSE temperatuuri tõusu kuni rõhuni 50 hPa. Samuti oli stsenaariumites, väljaarvatud 2050RCP4.5, märgata suhtelise õhuniiskuse tõusu kuni rõhuni 200 hPa. Arvestades muutusi meteoroloogilistes väljades, ei muutunud “tuleviku Gudrun” ühegi stsenaariumi korral intensiivsemaks ja tormitõus jäi umbkaudu samaks või vähenes. Kõige lähedasemad tulemused järelarvutustes tormitõusu kohta, olid vastavalt 2100 ja 2050RCP4.5 stsenaariumitel. Tuleviku simulatsioonides ja järelarvutuses esinesid teatud erinevused tuuletingimustes. Need variatsioonid võisid olla ka tormitõusu muutlikkuse põhjuseks. Lisaks näitas standardhälbe analüüs, et alla  $58^{\circ}$  laiuskraadi on suurte tuulte kiiruste hälve väike, kuid väiksemate kiiruste juures hälve tõuseb. Sellest saab järeldada, et tuleviku stsenaariumite vahel ei esinenu olulisi muutusi suurtes tuule kiirustes, mis oleksid võinud põhjustada suuremat veetaseme tõusu Pärnus.

Parasvöötme tsüklonite arengu eripära võib pidada põhjuseks, miks tormid ei tugevnenuud. Nimetatud tsükloniid ammutavad oma energia polaarfrondilt, kus puutuvad kokku külm ja soe õhumass ning väikesem temperatuuri gradient võib viia nõrgemate tormide kujunemisele. Kuna tegemist on üksiksündmuse arvutusega, ei saa selle põhjal tuleviku puudutavaid klimatoloogilisi üldistusi teha. Ebamäärasuste vähendamiseks on vajalik olemasolevat metoodikat edasi arendada ja läbi arvutada rohkem tormisündmusi, sealhulgas erinevatel aastaaegadel toimuvaaid ning erinevaid trajektoore pidi kulgevaid torme.

## **Acknowledgements**

The author of this study would like to thank Professor Tomoya Shibayama from Waseda University, under whose guidance the author learnt about the world of coastal engineering. The appreciation extends towards the entire Shibayama Lab and especially to Ryota Nakamura, who so kindly shared his knowledge in regards to atmospheric and ocean models. The author would like to recognise and thank PhD Ülo Suursaar for his kind assistance and guidance throughout the evolution of this research and also PhD Ain Kull for his constructive feedback and suggestions.

The study was financially supported by the Estonian Research Council grant PUT595 (to Ü.Suursaar).

## References

- Avotniece, Z., Rodinov, V., Lizuma, L., Briede, A., Klavins, M. (2010). Trends in the frequency of extreme climate events in Latvia. *Baltica* (23), 135–148.
- Beljaars, A.C.M. (1994). The parameterization of surface fluxes in large-scale models under free 530 convection. *Quarterly Journal of the Royal Meteorological Society* (121), 255–270
- Berz, G., Conrad, K. (1994). Stormy weather: the mounting windstorm risk and consequences for insurance industry. *Ecodesicion* (12), 65—69.
- Booth, J.F., Wang, S. and Polvani, L. (2013). Midlatitude storms in a moister world: Lessons from idealized baroclinic life cycle experiments. *Climate Dynamics* (41), 787-802
- Carpenter, G. (2005). Windstorm Erwin/ Gudrun – January 2005. Specialty Practice Briefing, 2.
- Chang E.K.M., Guo, Y. and Xia, X. (2012). CMIP5 multimodel ensemble projection of storm track change under global warming. *J. Geophys. Res.* 117 (D23)D23118
- Chen, C., Liu, H., Beardsley, R.C. (2003). An Unstructured Grid, Finite-Volume, Three-Dimensional, Primitive Equations Ocean Model: Application to Coastal Ocean and Estuaries. *Journal of Atmospheric and Oceanic Technology* (20), 159–186.
- Christensen, J.H., K. Krishna Kumar, E. Aldrian, S.-I. An, I.F.A. Cavalcanti, M. de Castro, W. Dong, P. Goswami, A. Hall, J.K. Kanyanga, A. Kitoh, J. Kossin, N.-C. Lau, J. Renwick, D.B. Stephenson, S.-P. Xie and T. Zhou, 2013: Climate Phenomena and their Relevance for Future Regional Climate Change. In: *Climate Change 2013: The Physical Science Basis. Contribution of Working Group I to the Fifth Assessment Report of the Intergovernmental Panel on Climate Change* [Stocker, T.F., D. Qin, G.-K. Plattner, M. Tignor, S.K. Allen, J. Boschung, A. Nauels, Y. Xia, V. Bex and P.M. Midgley (eds.)]. Cambridge University Press, Cambridge, United Kingdom and New York, NY, USA.
- Collins, M., R. Knutti, J. Arblaster, J.-L. Dufresne, T. Fichefet, P. Friedlingstein, X. Gao, W.J. Gutowski, T. Johns, G. Krinner, M. Shongwe, C. Tebaldi, A.J. Weaver and M. Wehner, 2013: Long-term Climate Change: Projections, Commitments and Irreversibility. In: *Climate Change 2013: The Physical Science Basis. Contribution of Working Group I to the Fifth Assessment Report of the Intergovernmental Panel on Climate Change* [Stocker, T.F., D. Qin, G.-K. Plattner, M. Tignor, S.K. Allen, J. Boschung, A. Nauels,

Y. Xia, V. Bex and P.M. Midgley (eds.)]. Cambridge University Press, Cambridge, United Kingdom and New York, NY, USA.

Dyer, A.J., Hicks, B.B. (1970). Flux-gradient relationships in the constant flux layer.

Quarterly Journal of the Royal Meteorological Society (96), 715–721.

Eelsalu, M., Soomere, T., Pindsoo, K., Lagemaa, P. (2014). Ensemble approach for projections of return periods of extreme water levels in Estonian waters. *Continental Shelf Research* (91), 201–210.

Emanuel, K. (2005). Increasing destructiveness of tropical cyclones over the past 30 years. *Nature* (436), 686–688.

Feser, F., Barcikowska, M., Krueger, O., Schenk, F., Weisse, R., Xia, L. (2015). Storminess over the North Atlantic and northwestern Europe – A review. *Quarterly Journal of the Royal Meteorological Society* (141), 350–382.

Hansen, J., Sato, M., Hearty, P., Ruedy, R., Kelley, M., Masson-Delmotte, V., Russell, G., Tselioudis, G., Cao, J., Rignot, E., Velicogna, I., Tormey, B., Donovan, B., Kandiano, E., von Schuckmann, K., Kharecha, P., Legrande, A.N., Bauer, M., Lo, K.-W. (2016). Ice melt, sea level rise and superstorms: evidence from paleoclimate data, climate modeling, and modern observations that 2°C global warming could be dangerous. *Atmospheric Chemistry and Physics* (16), 3761–3812.

Harvey, B. J., Shaffrey L C, Woollings, T. J., Zappa, G. and Hodges, K. I. (2012). How large are projected 21st century storm track changes? *Geophysical Research Letters* (39), 1–5

Hill, D., (2012). The lessons of Katrina, learned and unlearned. *Journal of Coastal Research* (29), 324–331.

Hong, S.Y., Lim, J.O.J. (2006). The WRF single-moment 6-class microphysics scheme (WSM6). *Journal of The Korean Meteorological Society* (42), 129–151.

Hong, S.Y., Noh, Y., Dudhia, J. (2006). A new vertical diffusion package with an explicit treatment of entrainment processes. *Monthly Weather Review* (134), 2318–2341.

Jaagus J. (2006). Climatic changes in Estonia during the second half of the 20th century in relationship with changes in large-scale atmospheric circulation. *Theoretical and Applied Climatology* (83), 77-88.

Jaagus, J., Kull, A. (2011). Changes in surface wind directions in Estonia during 1966-2008 and their relationships with large-scale atmospheric circulation. *Estonian Journal of Earth Sciences* (60), 220–231.

- Jaagus, J., Suursaar, Ü. (2013). Long-term storminess and sea level variations on the Estonian coast of the Baltic Sea in relation to large-scale atmospheric circulation. *Estonian Journal of Earth Sciences* (62), 73–92.
- Bader, J., Mesquita, M.D.S., Hodges, K.I., Keenlyside, N., Østerhus, S., Miles, M. (2011). A review on Northern Hemisphere sea-ice, storminess and the North Atlantic Oscillation: Observations and projected changes. *Atmospheric Research* (101), 809–834.
- Knippertz, P., Ulbrich, U. and Speth, P. (2000). Changing cyclones and surface wind speeds over the North Atlantic and Europe in a transient GHG experiment. *Climate Research* (15), 109–122.
- Lehmann A., Getzlaff K., Harlaß J. (2011). Detailed assessment of climate variability in the Baltic Sea area for the period 1958 to 2009. *Climate Research* (46), 185–196.
- Mizuta, R. (2012). Intensification of extratropical cyclones associated with the polar jet change in the CMIP5 global warming projections. *Geophysical Research Letters* (39), L19707.
- Nakamura, R., Iwamoto, T., Shibayama, T., Mikami, T., Matsuba, S., Mäll, M., Takekouji, A., Tanokura, Y. (2015a). Field survey and mechanism of storm surge generation invoked by the low pressure with rapid development in Nemuro Hokkaido in December 2014. *Journal of Japan Society of Civil Engineers* (71), 31–36.
- Nakamura, R., Shibayama, T., Esteban, M., Iwamoto, T. (2016). Future typhoon and storm surges under different global warming scenarios: case study of typhoon Haiyan (2013). *Natural Hazards*, 1–37.
- Nakamura, R., Takahiro, O., Shibayama, T., Esteban, M., Takagi, H. (2015b). Evaluation of storm surge caused by typhoon Yolanda (2013) and using weather – Storm surge – Wave – Tide model. *Procedia Engineering* (116), 373–380.
- NCEP FNL. (2000). National Centers for Environmental Prediction/National Weather Service/NOAA/U.S. Department of Commerce: NCEP FNL Operational Model Global Tropospheric Analyses, continuing from July 1999. Research Data Archive at the National Center for Atmospheric Research, Computational and Information Systems Laboratory. Accessed 10 Jan 2015.
- Paulson C.A. (1970). The mathematical representation of wind speed and temperature profiles in the unstable atmospheric surface layer. *Journal of Applied Meteorology* (9), 857–861.

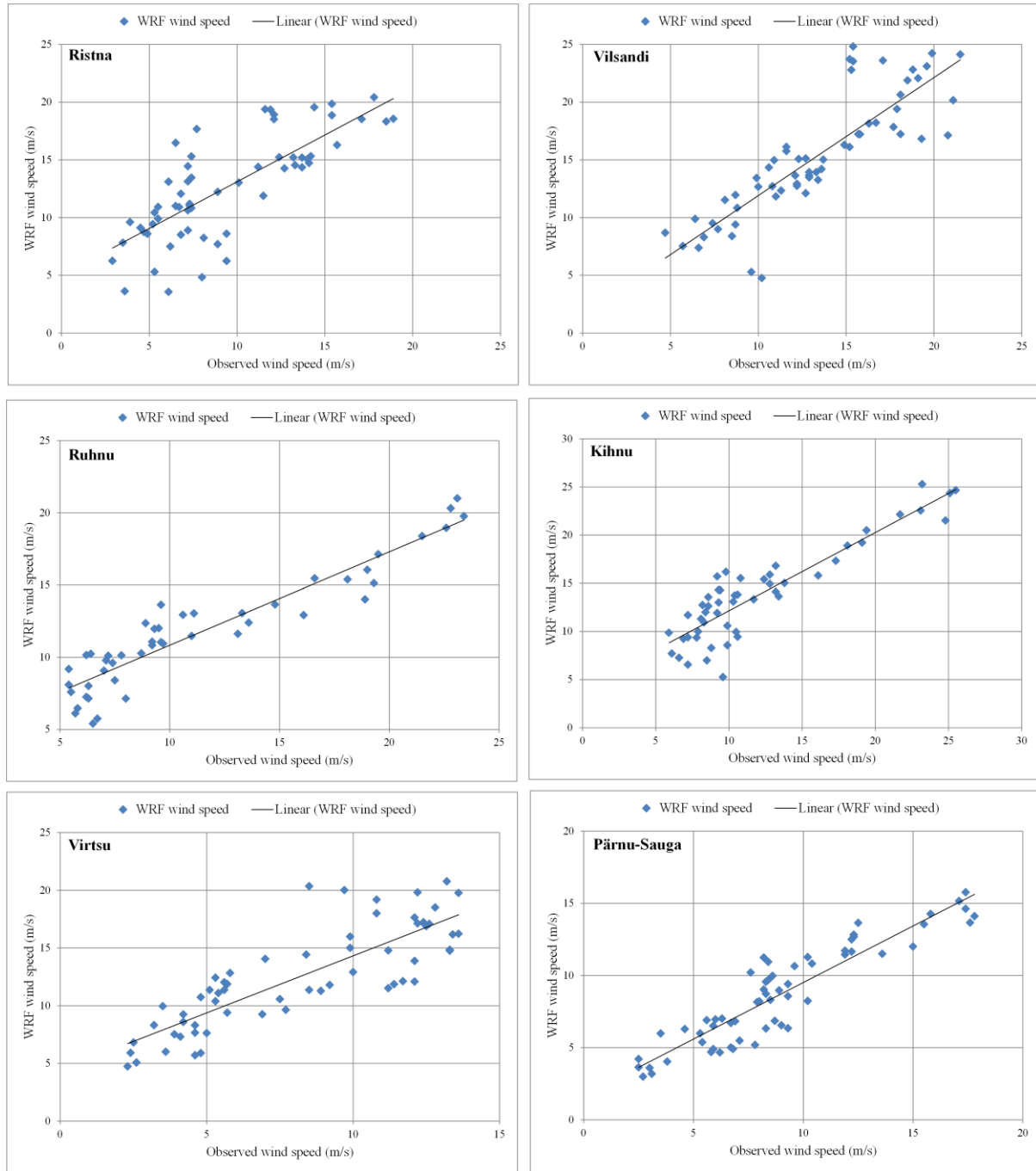
- Pinto, J.G., Ulbrich, U., Leckebusch, G.C, Spangehl, T., Reyers, M., Zacharias, S., (2007). Changes in storm track and cyclone activity in three SRES ensemble experiments with the ECHAM5/MPI-OM1 GCM. *Climate Dynamics* (29), 195–210.
- Post, P., Kõuts, T. (2014). Characteristics of cyclones causing extreme sea levels in the northern Baltic Sea. *Oceanologia* 56(S), 241–258.
- Roberts, J.F., Champion, A.J., Dawkins, L.C., Hodges, K.I., Shaffrey, L.C., Stephenson, D.B., Stringer, M.A., Thornton, H.E., Youngman, B.D. (2014). The XWS open access catalogue of extreme European windstorms from 1979 to 2012. *Natural Hazards and Earth System Sciences*, (14), 2487–2501.
- Rutgersson, A., Jaagus, J., Schenk, F., Stendel, M., Bärring, L., Briede, A., Claremar, B., Hanssen-Bauer, I., Holopainen, J., Moberg, A., Nordli, Ø., Rimkus, E., Wibig, J. (2015). Recent change – atmosphere. In: The BACC II Author Team (Ed.). *Second Assessment of Climate Change for the Baltic Sea Basin*, pp. 69–97, Springer.
- Schmidt, H., von Storch, H. (1993). German Bight storms analysed. *Nature* (365), 791.
- Sepp, M.; Post, P.; Jaagus, J. (2005). Long-term changes in the frequency of cyclones and their trajectories in Central and Northern Europe. *Nordic Hydrology* (36), 297–309.
- Shibayama, T. (2015). Field surveys of recent storm surge disasters. *Procedia Engineering* (116), 179–186.
- Skamarock, W.C., Klemp, J.B., Dudhia, J., Gill, D.O., Barker, D.M., Duda, M.G., Huang, X.Y., Wang, W., Powers, J.G. (2008). A Description of the Advanced Research WRF Version 3, NCAR Technical Note.
- Soomere, T.; Behrens, A.; Tuomi, L.; Nielsen, J.W. (2008). Wave conditions in the Baltic Proper and in the Gulf of Finland during windstorm Gudrun. *Natural Hazards and Earth System Sciences* (8), 37–46.
- Suursaar, Ü., Jaagus, J., Tõnisson, H., (2015). How to quantify long-term changes in coastal sea storminess? *Estuarine Coastal and Shelf Science* (156), 31–41.
- Suursaar, Ü., Kullas, T., Otsmann, M., Kõuts, T. (2003). Extreme sea level events in the coastal waters of western Estonia. *Journal of Sea Research* (49), 295–303.
- Suursaar, Ü., Kullas, T., Otsmann, M., Saaremäe, I., Kuik, J., Merilain, M. (2006). Hurricane Gudrun and modelling its hydrodynamic consequences in the Estonian coastal waters. *Boreal Environment Research* (11), 143–159.
- Suursaar, Ü., Sooäär, J. (2006). Storm surge induced by extratropical cyclone Gudrun: hydrodynamic reconstruction of the event, assessment of mitigation actions and analysis of future flood risks in Pärnu, Estonia. In: Brebbia, C.C.; Popov, V: (Ed.). *Risk*

Analysis V: Simulation and Hazard Mitigation (241–250). WIT Press. (WIT Transactions on Ecology and the Environment; 91).

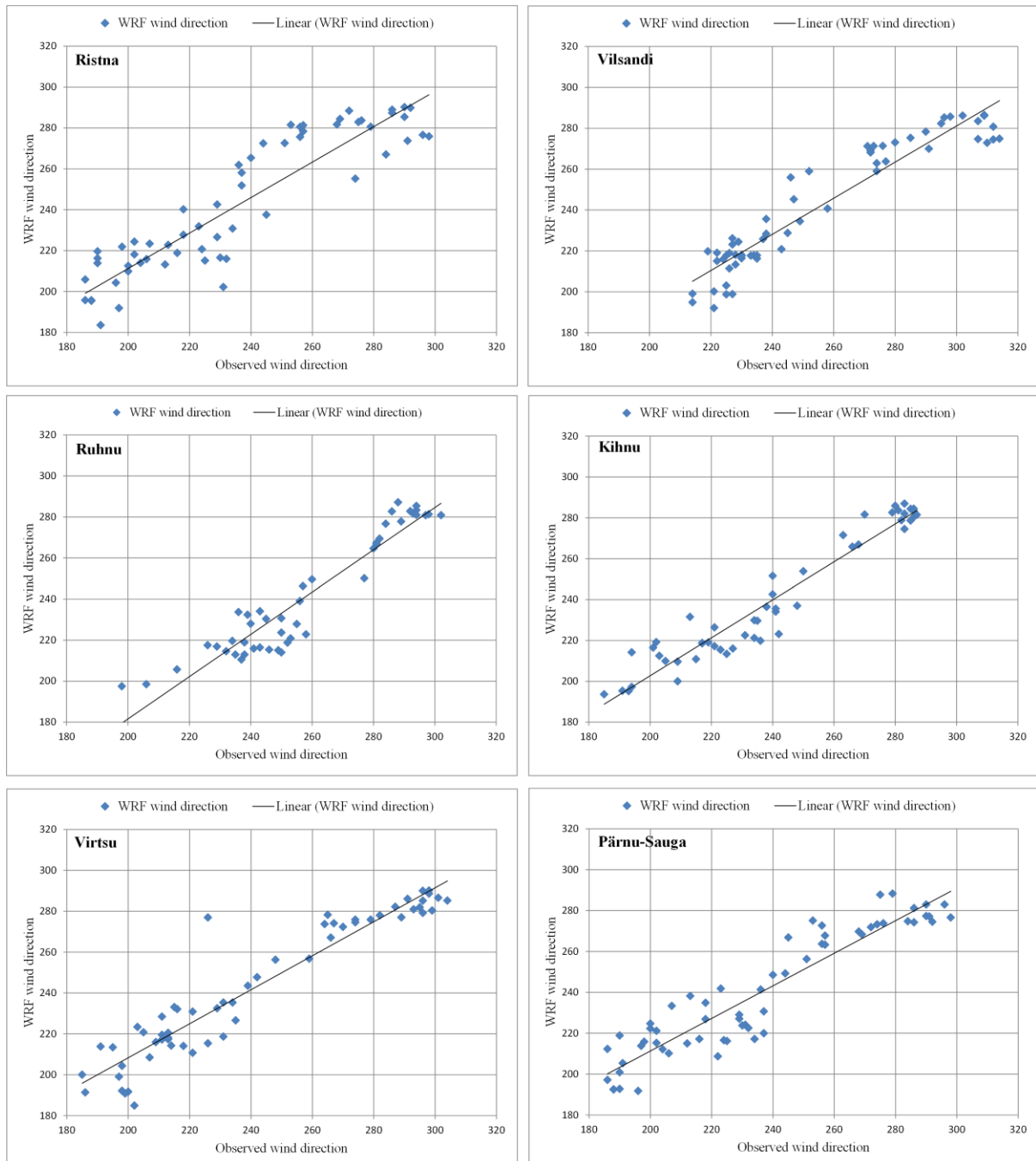
- Suursaar, Ü., Tõnisson, H., Alari, V., Raudsepp, U., Rästas, H., Anderson, A. (2016). Projected changes in wave conditions in the northern Baltic Sea by the end of 21th century and the corresponding shoreline changes. *Journal of Coastal Research*, Special Issue No. 75 (in press).
- Tasnim, K.M., Shibayama, T., Esteban, M., Takagi, H., Ohira, K., Nakamura, R. (2015). Field observation and numerical simulation of past and future storm surges in the Bay of Bengal: case study of cyclone Nargis. *Natural Hazards* (75), 1619–1647.
- Tewari, M., Chen, F., Wang, W., Dudhia, J., LeMone, M.A., Mitchell, K., Ek, M., Gayno, G., Wegiel, J., Cuenca, R.H. (2004). Implementation and verification of the unified NOAH land surface 677 model in the WRF model. 678 20th conference on weather analysis and forecasting/16th conference on numerical weather prediction (679), 11–15.
- Trenberth, K., (2005). Uncertainty in hurricanes and global warming. *Science* (308), 1753–1754.
- Tõnisson, H., Orviku, K., Jaagus, J., Suursaar, Ü., Kont, A., Rivis, R. (2008). Coastal damages on Saaremaa Island, Estonia, caused by the extreme storm and flooding on January 9, 2005. *Journal of Coastal Research* (24), 602–614.
- Ulbrich, U., Leckebusch, G.C., G. Pinto, J.G. (2009). Extra-tropical cyclones in the present and future climate: A review. *Theoretical and Applied Climatology* (96), 117–131.
- Ulbrich, U., Pinto, J.G., Kupfer, H., Leckebusch, G.C., Spangehl, T., Reyers, M. (2008). Changing northern hemisphere storm tracks in an ensemble of IPCC climate change simulations. *Journal of Climate* (21), 1669–1679.
- Watanabe, M., Suzuki, T., O’ishi, R., Komuro, Y., Watanabe, S., Emori, S., Takemura, T., Chikira, M., Ogura, T., Sekiguchi, M., Takata, K., Yamazaki, D., Yokohata, T., Nozawa, T., Hasumi, H., Tatebe, H., Kimoto, M. (2010). Improved Climate Simulation by MIROC5: Mean States, Variability, and Climate Sensitivity. *Jounral of Climate* (23), 6312–6335.
- Webb, E.K. (1970). Profile relationships: The log-linear range, and extension to strong stability. *Quarterly Journal of the Royal Meteorological Society* (96), 67–90.
- Webersik, C., Esteban, M., Shibayama, T. (2010). The economic impact of future increase in tropical cyclones in Japan. *Natural Hazards* (55), 233–250.

- Woollings, T., Gregory, J.M., Pinto, J.G., Reyers, M., Brayshaw, D.J. (2012). Response of the North Atlantic storm track to climate change shaped by ocean–atmosphere coupling. *Nature Geoscience* (5), 313–317
- Zappa G., Shaffrey L.C., Hodges K.I., Sansom P.G., Stephenson D.B. (2013). A multi-model assessment of future projections of north atlantic and european extratropical cyclones in the CMIP5 climate models. *Journal of Climate* (26) 5846–5862.
- Zhang, D.L., Anthes, R.A. (1982). A high-resolution model of the planetary boundary layer—sensitivity tests and comparisons with SESAME-79 data. *Journal of Applied Meteorology* (21), 1594–1609.

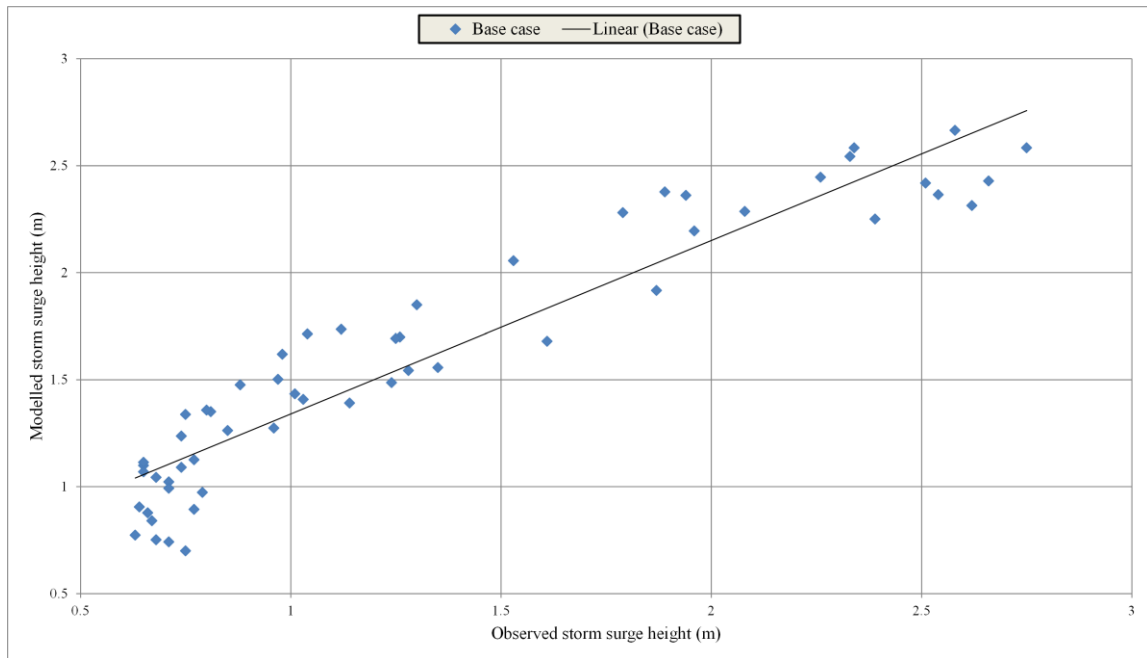
## Appendices



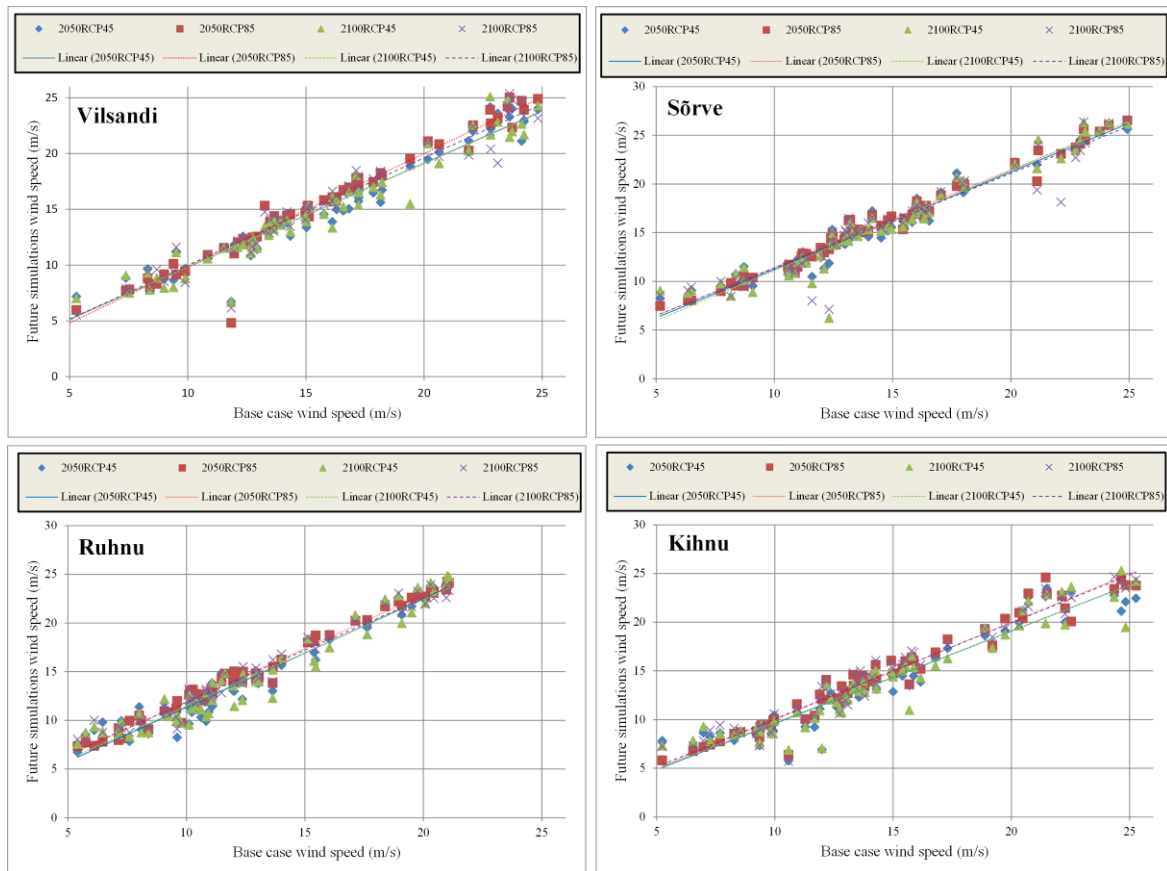
**Appendix 1.** Base case and observation wind speed relationships for 6 weather stations.



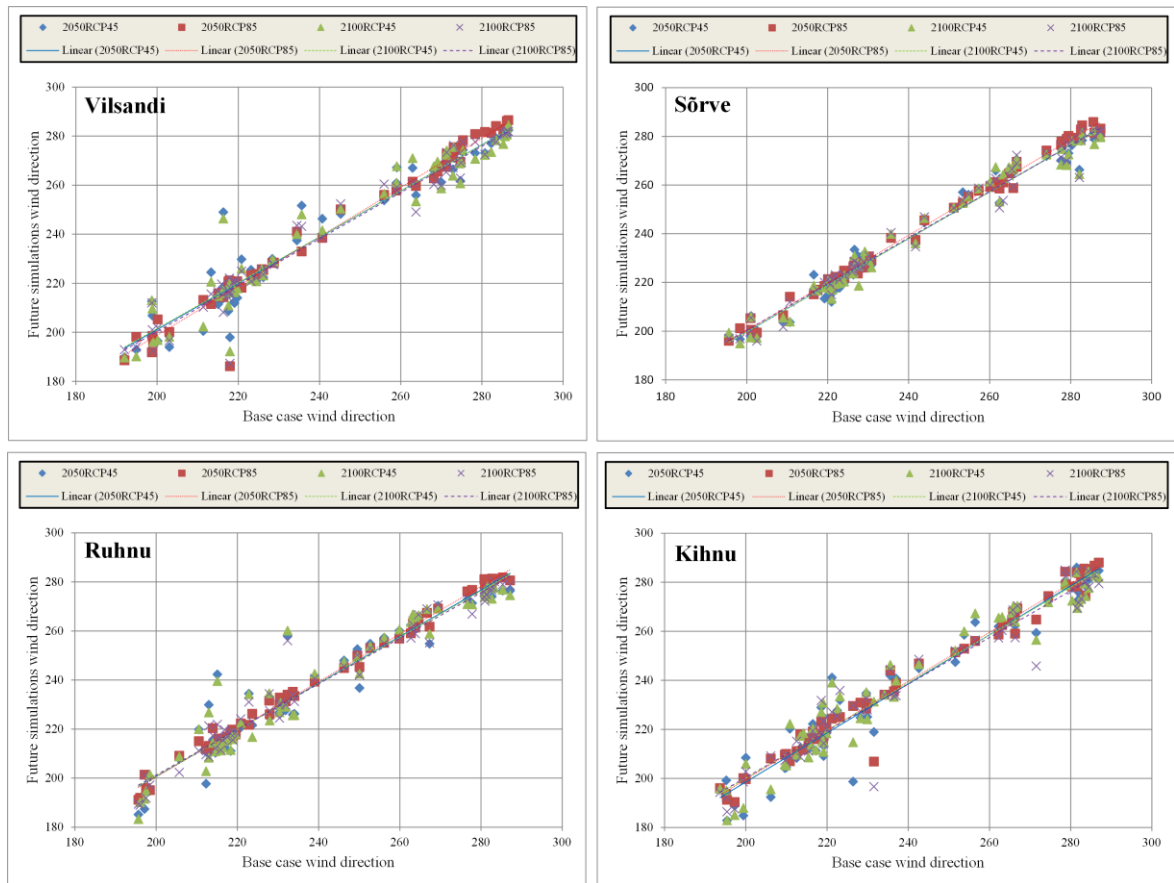
**Appendix 2. Base case and observations wind direction relationships for 6 weather stations.**



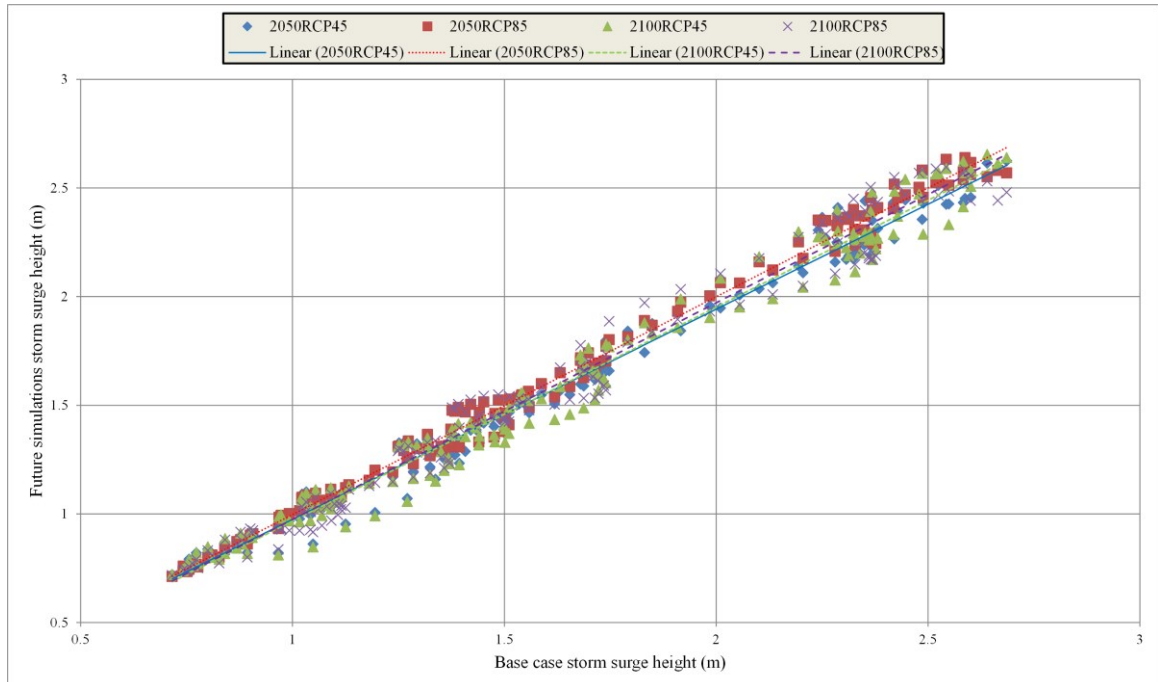
**Appendix 3.** Simulation and observation surge height relationship at Pärnu tide gauge.



**Appendix 4.** Base case and future scenarios wind speed relationships for 4 weather stations.



**Appendix 5.** Base case and future scenarios wind direction relationships for 4 weather stations.



**Appendix 6.** Base case and future scenarios for surge height relationships at Pärnu tide gauge.

## **Published/ accepted publications**

- Article 1. Mäll, M., Nakamura, R., Shibayama, T., Suursaar, Ü., Kull, A. (2016a). Tulevikutormide simuleerimine kasutades atmosfääri- (WRF) ja ookeanimudelit (FVCOM) 2005. aasta jaanuaritormi (Gudrun) näitel. In: Teaduskonverents METOBS 150 (2-3.dets.2015, Tõravere) kogumik. Publicationes Geophysicales Universitatis Tartuensis. 10 p. (in press).
- Article 2. Mäll, M., Nakamura, R., Shibayama, T., Suursaar, Ü., Kull, A. (2016b). Modelling a storm surge under future climate scenarios: case study of storm Gudrun. In: 35th International Conference on Coastal Engineering (ICCE2016), 17-22. July 2016, Istanbul, Turkey. Abstracts (in press).
- Article 3. Nakamura, R., Iwamoto, T., Shibayama, T., Mikami, T., Matsuba, S., Maell, M., Takekouji, A., Tanokura, Y. (2015). Field survey and mechanism of storm surge generation invoked in Nemuro Hokkaido in December 2014. Journal of Japan Society of Civil Engineers (71), 31–36.

# **Tulevikutormide simuleerimine, kasutades atmosfääri- (WRF) ja ookeanimudelit (FVCOM) 2005. aasta jaanuaritormi (Gudrun) näitel**

Martin Mäll

*Tartu Ülikooli Ökoloogia- ja Maateaduste Instituut*

Ryota Nakamura, Tomoya Shibayama

*Waseda Ülikooli Tsivil- ja Keskkonnatehnika osakond (Jaapan)*

Ülo Suursaar

*Tartu Ülikooli Eesti Mereinstituut*

Ain Kull

*Tartu Ülikooli Ökoloogia- ja Maateaduste Instituut*

## **1. Sissejuhatus**

Kaasaegse kliimamuutuse (nn globaalse soojenemise) üheks ohtlikuks kaasnähuks peetakse tormisuse kasvu, mis koos globaalse meretaseme tõusuga ohustab laialdasi rannikualasid, näiteks Madalamaades, Kagu-Aasias, Mehiko lahe piirkonnas ja mujal (Emanuel, 2005). Rääkides „tormisuse kasvust”, tuleb siiski vahet teha, kas tormid muutuvad sagedasemaks, intensiivsemaks või mõlemat. Kuigi on avaldatud arvamust, et ookeanipinna soojenemine peaks esile kutsuma eelkõige troopiliste tormide (Knutson & Tuleya, 2004) ja võimalik, et ka paravöötme tsüklonite intensiivistumist või sageduse kasvu (Leckebusch & Ulbrich, 2004; Hansen jt., 2016), ei ole seda paljude teiste uurijate arvates praegu siiski võimalik kindlalt väita (Schmidt & von Storch, 1993; Trenberth, 2005). Ühelt poolt on tsüklonaalsuse loomulik muutlikkus väga suur (Rutgersson jt., 2015) ning teiselt poolt on suur ka atmosfääri tulevikustsenariumide hajuvus ja seda just tuulte ja tormide osas (Christensen jt., 2015). Ka inimkonnale põhjustatud kannatuste ja majandusliku (või kindlustus-) kahju vaiydamatu tõus (Berz & Conrad, 1994; Webersik jt., 2010) ei pruugi peegeldada mitte ainult tormisuse kui geofüüsikalise nähtuse trendi, vaid ka rannikualade üha intensiivsemat majanduslikku kasutuselevõttu ning sealsete rahvaarvu pidevat kasvu. Samuti ei ole tormisuse kasv kindlasti kõikehõlmav ja kõikjal ühetaoliselt kulgev protsess (Feser jt., 2014).

Tsüklonite kujunemine ja areng kulgeb troopilistel ja suurematel laiuskraadidel erinevalt ning erinevad on ka tormide iseloom, parameetrid ja mõjud. Suurimat globaalset vastukaja on saanud võimsad troopilised tsüklonid (orkaanid, taifuunid), nagu Katrina (2005, Mehiko laht), Nargis (2008, Bengali laht), Sandy (2012, USA idarannik) ja Haiyan/Yolanda (2013, Filipiinid). Neid torme on uuritud erinevate uurimisrühmade poolt (Hill, 2012; Shibayama, 2015; Nakamura jt., 2016), kasutades erinevaid mudeleid ning algtingimusi, sealhulgas ka selliseid, mis lubaksid heita valgust küsimusele, milline võiks olla „tuleviku Haiyan” või „tuleviku Nargis”.

Ka Läänemere piirkonnas võib kliimamuutusega seotud ohuks pidada tormisuse kasvu ja tormidega kaasnevate üleujutuste suurenemist (Avotniece jt., 2010; Suursaar jt., 2015). Üleujutuste oht suureneb osalt seetõttu, et globaalse meretaseme tasapisi kiirenev tõus on seni veel olnud suuresti kompenseeritud jääajajärgse maakerkega Läänemere põhja- ja kirdeosas, mis aga omakorda pidevalt aeglustub. Niisiis kujutavad klimaatilistest teguritest Läänemere regioonis suurimat ohtu paravöötme (ekstratropilised, mittetroopilised, tropikavälised) tsüklonid. Sellised tormid arenevad tavaliselt sügis-talvisel ajal Atlandi ookeani põhjaosas Islandi, Gröönimaa ning Newfoundlandi poolsaare vahelisel alal polaarfrondi läheduses. Seega sellised tsüklonid, erinevalt troopikas sündivatest tsüklonitest, omandavad oma energia kahel pool polaarfronti asuvate suurte õhumasside erinevusest, peamiselt temperatuurierinevustest. Läänetuulte vööndis Läänemere suunas liikudes võivad need tormid siin, aga ka Briti saartel, Skandinaavias ja mujalgi Põhja-Euroopas suurt kahju teha (Post & Kõuts, 2014). Viimase paari aastakümne olulisemad tormid Lääne Euroopas XWS-i tormisuse kataloogi andmetel (Roberts jt., 2012) on olnud 87J (oktoober 1987), Daria (jaanuar 1990), Vivian (veebruar 1990), Anatol (detsember 1999), Gudrun/Erwin (jaanuar 2005) ja Kybil (jaanuar 2007). Võib tödeda, et erinevad meteoroloogilised indeksid annavad pisut erinevaid tulemusi. Kuna Läänemere põhja-lõunasuunaline ulatus on suur (ligi 1400 km) ning tormide lokaalne mõju rannikualadele sõltub

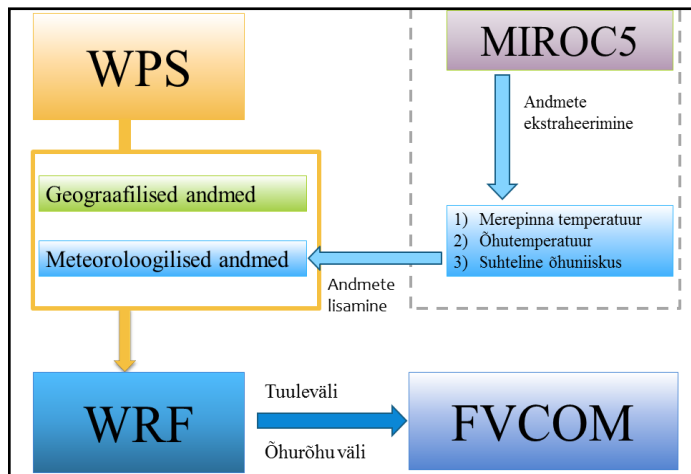
tugevalt trajektoorist, siis on ka Eesti rannikumerd kõige enam mõjutanud tormide nimikiri osaliselt erinev (Jaagus & Suursaar, 2013; Suursaar jt., 2015): Gudrun/Erwin (9. jaanuar 2005), tormid 2. novembril 1969, 18. oktoobril 1967, 17. detsembril 1990, 1. novembril 2001, 22. veebruaril 1990, ning St. Jude (29. oktoobril 2013). Suurima mõjuga ja ekstreemseim oli 2005. aasta jaanuaritorm Gudrun/Erwin, mis põhjustas rannikulinnades rekordtasemel üleujutusi. Pärnu linnas olev mareograaf mõõtis veetaseme tõusuks +275 cm üle nulli, kus nulltase vastab umbkaudu pikaajalisele keskmisele veetasemele. Torm ja kaasnenuud üleujutus tekitasid olulist majanduslikku kahju ning rannapurustusi (Suursaar jt., 2006; Tõnisson jt., 2008).

Seoses viimastel aastakümnetel intensiivlistunud rannikuerosiooni (Orviku jt., 2003) ja teiste tormikahjustustega on oluline paremini mõista tulevikus esineda võivaid torme ja nende mõjud Eesti kontekstis. Kas Lääänemere tormid muutuvad tulevikus tõusva temperatuuri foonil tugevamaks? Kas üleujutused sagenevad, arvestades globaalset meretõusu (Eelsalu jt., 2014)? Selle uurimistöö eesmärk on järelprognoosina modelleerida torm Gudrun, kasutades selleks atmosfäärimudelit Weather Research & Forecasting (ARW-WRF) ja ookeanimudelit Finite Volume Community Ocean Model (FVCOM). Need mudelid, mida kirjeldatakse lähemalt allpool, on leidnud kasutust mitmetes maades, sealhulgas Jaapanis Waseda ülikooli nn Shibayama laboris (Nakamura jt., 2015; 2016; Shibayama, 2015; Tasnim jt., 2015). „Tuleviku Gudrunid” arvutatakse, arvestades Valitsustevahelise Kliimamuutuste Paneeli viendas hindamisraportis (IPCC AR5) toodud kliimamuutuste stsenaariume RCP4.5 ja RCP8.5 (RCP – Representative Concentration Pathways), keskendudes aastatele 2050 ja 2100.

## 2. Metoodika

Mudelite süsteem on kujutatud joonisel 1 (Nakamura jt., 2016). Simuleerimiseks kasutati nn ülalt alla ehk jada-lähenemist, kus atmosfäärimudel töötab esimesena ja selle väljundit kasutakse sisendina ookeanimudelile. Atmosfäärimudel WRF on numbriline, operatiivset ilmaprognosi võimaldav keskmise mõõtkava (mesoskaala) mudel, mida on alates 1990ndatest areandanud mitmeid USA uurimisasutusi (NCAR, NOAA, AFWA, NRL jt.) ning ülikoole hõlmav konsortsium. Idealiseeritud tingimustel või reaalsete assimileeritud vaatlusandmete alusel on WRF võimeline piisavalt täpselt simuleerima atmosfääritingimusi nii teadustöö kui ka reaalajaliste prognooside jaoks (Skamarock jt., 2008). Mudeli registreeritud kasutajaid leidub juba enam kui 150 riigis. Selles töös tehti WRF-i mudeliga arvutusi kolmes Lääne-Eesti rannikumerele keskenduvas modeleerimispiirkonnas (joonis 2) 2005. a Gudruni tormi toimumise eel ja järel. Arvutuse kestus esimesel modeleerimisalal oli 96 h, teisel 84 h ja kolmandal 60 h. Kontrollsimulatsiooni meteoroloogiliste väljade sisendandmed saadi USA NCEP (National Centre for Environmental Protection) operatiivanalüüsist (<http://rda.ucar.edu/>).

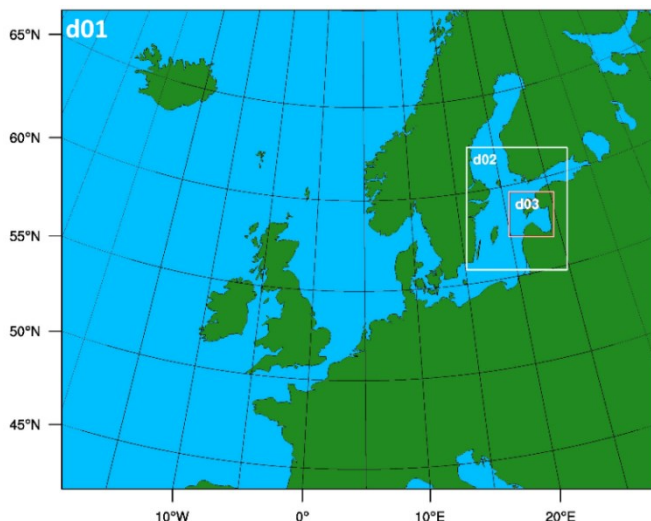
Tulevikustsenuuriumide saamiseks asendati algsed NCEP järelarvutuse merepinna veetemperatuuri, õhutemperatuuri ja suhtelise õhuniiskuse andmed MIROC5 mudeli abil saadud tuleviku jaoks manipuleeritud andmetega. Nagu töös Tasnim jt. (2015), erinesid ka meie tuleviku sisendväljad nimetatud kolme parameetri osas, kuid põhimõtteliselt võib neid erinevust tekitavad parameetreid MIROC5 baasist ekstraheerida teisigi. Tuleviku simulatsioonide jaoks kasutatud kliimamudel MIROC5 (Model for Interdisciplinary Research on Climate) on CMIP5 (Coupled Model Intercomparison Project, Phase 5) raames Jaapani teadlaste (Watanabe jt., 2010) loodud globaalne mudel, mille arvutusi on muu hulgas laialdaselt kasutatud ka IPCC tulevikustsenuuriumide juures. Selles töös arvestati IPCC AR5 raportis toodud RCP4.5 ja RCP8.5 stsenaariumidel põhinevaid kliimaprojektsioone. Valitud stsenaariume (RCP4.5 ja RCP8.5) käsitletakse aastatel 2050 ja 2100, kus vajalikud parameetrite väärтused saadi aastate 2045–2055 ja 2091–2100 keskmistatud väärтustest. Saadud tuleviku ja oleviku erinevus interpoleeriti (uuritava kuu, jaanuari kohta) kõikidele WRF-i simuleeritud meteoroloogilistele võrgupunktidele ja vertikaalsetele tasemetele. Need võrgupunktid on algsest koostatud WRF-i eeltöötlusprogrammiga WPS, kasutades NCEP FNL-i andmestikku. Näiteks erinesid merepinna keskmised temperatuurid stsenaariumidel 2050RCP4.5, 2100RCP4.5, 2050RCP8.5 ja 2100RCP8.5 vastavalt 0,25; 1,16; 1,22 ja 2,8 K võrra kontrollperioodi 2006–2011 suhtes.



**Joonis 1.** Kasutatud mudelite plokk-skeem tormi ja veetaseme muutuse modelleerimiseks.

**Figure 1.** Flowchart of models used for storm surge modelling.

Tsüklonit sisaldavat atmosfääritingimuste kontrollsimulatsiooni ja stsenaariumiarvutusi kasutati ookeanimudeli arvutustes, kus põhitähelepanu keskendus veetaseme väljade muutumisele. Kolmemõõtmeline ookeani prognoosmudel FVCOM on struktureerimata võrguga nn avatud kogukonnamudel, mille lõid algsest USA Woods Hole'i Okeanoloogia Instituudi ja Massachusettsi Ülikooli Dartmouthi teadlased (<http://fvcom.smast.umassd.edu/fvcom/>). Mudeli pidevalt edasiarendatav merefüüsikaline sisu ning topoloogiline paindlikkus teevad FVCOM-ist ranniku uuringutes ja interdisciplinaartsetes rakendustes laialtlevinud tööriista (Chen jt., 2003). Siinnes uuringus oli mudeli arvutuste kestus kõige väiksemal modelleerimisalal (do3; joonis 3) 54 h. Mudelites kasutatud andmed ja parameetrite valikud on esitatud tabelis 1. Nii atmosfääri kui ka mere hüdrodünaamiliste parameetrite lähteolukorra järelarvutuse (*hindcast*) tulemuste võrdluseks kasutati Eesti Keskkonnaagentuurilt saadud tunnise intervalliga tuule kiiruse, suuna ja veetaseme vaatlusandmeid valitud rannalähedatest jaamadest (joonis 3).



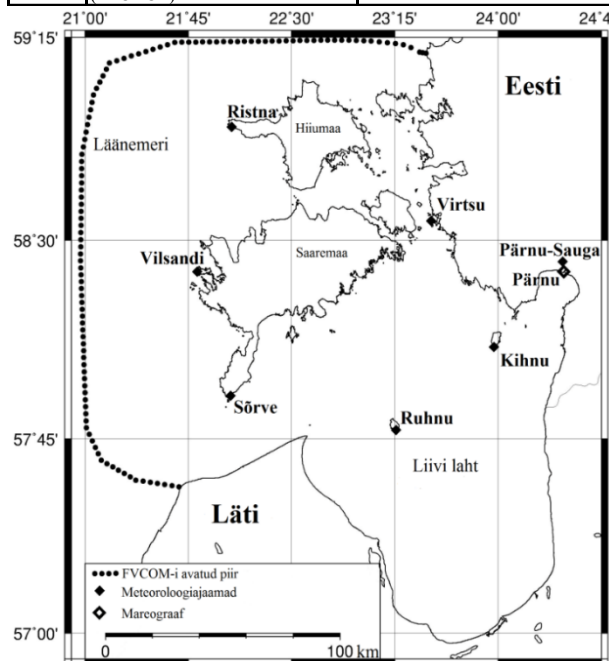
**Joonis 2.** WRF-i atmosfäärimudelis kasutatud kolm järjestikust modelleerimisala.

**Figure 2.** Nested domains (d01, do2, do3) used in the WRF atmosphere model.

**Tabel 1.** Mudelite alg- ja ääretingimused.

**Table 1.** Initial and boundary conditions for used models.

	Nimekiri	Valikud
WRF	Simulatsiooni aeg (domeen 1)	18:00 UTC 06/01/2005 – 18:00 UTC 10/01/2005
	Simulatsiooni aeg (domeen 2)	06:00 UTC 07/01/2005 – 18:00 UTC 10/01/2005
	Simulatsiooni aeg (domeen 3)	06:00 UTC 08/01/2005 – 18:00 UTC 10/01/2005
	Võrgusamm (domeen 1)	22.5 km
	Võrgusamm (domeen 2)	4.5 km
	Võrgusamm (domeen 3)	0.9 km
	Õhurõhu ülempuur	50 hPa
	Kihte vertikaalis	27
	Domeene	3
	Pesitsusiskeem	kahesuunaline
	Mikrofütüsika	WSM6
	Pinnakiht	Revised MM5 Monin-Obukhov scheme
	Maapind	Unified Noah land-surface model
	Planetaarne	YSU
	Projektsioon	Lamberti Konformne kooniline
	Merestügavuse andmed	USGS
	Atmosfääri andmed	NCEP FNL Operational Global Analysis
	Atmosfääri andmete resolutsioon	1 x 1 kraadi
FVCOM	Simulatsiooni aeg	06:00 UTC 08/01/2005 – 12:00 UTC 10/01/2005
	Noode	63 189
	Elementide arv	123 533
	Võrgusilma suurus	50 m – 2000 m
	Kõrgusandmed	DEM - 5 m, SRTM90 - 90 m,ETOPO1 - 1 arc-minut
	Rannikumere sügavusandmed (Veeteede Amet)	Pärnu laht ja jõgi - 5 m; Liivi laht, Väinameri, Irbe Väin - 50m
	Rannikumere sügavusandmed (ETOPO1)	1 arc-minut



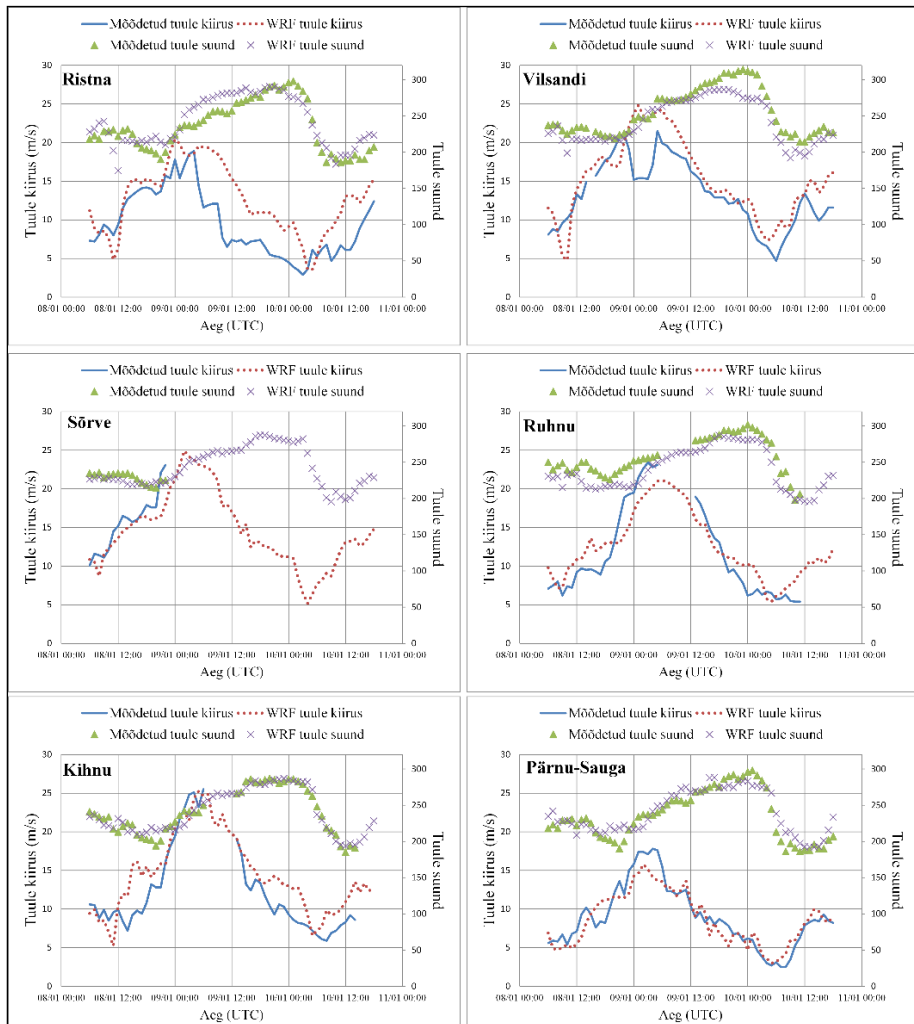
**Joonis 3.** FVCOM-i uurimisala, mis jäab WRF-i modelleerimisala do3 (joonis 2) alla.  
**Figure 3.** Study area of the FVCOM which falls under the WRF domain 3 (Figure 2).

### 3. Gudruni järelarvutuse tulemused

Mõõtmiste järgi ulatus ilmajaamades 10 minuti keskmise tuule kiirus 9. jaanuaril 2005 tormi Gudrun ajal kuni 28 meetrini sekundis (Sõrves) ning puhangud ulatusid 38 meetrini sekundis (Kihnu); paljudes veemõõdupostides mõõdeti uued meretaseme rekordid. Samas on teada, et tormi tõttu esines häireid või katkestusi mitme ilmajaama töös (sh Vilsandil, Ruhnus) ja mitme merejaama veetaseme andmed olid puudu või moonutatud (Ristna). Seetõttu tuli hiljem mitmeid tormi-

parameetriteid hinnata mudelite abil (Suursaar jt., 2006). Selles töös võrreldi järelarvutuste tulemusi kuues ilmajaamas mõõdetud väärustega, kusjuures eespool mainitud tormist tingitud tehniliste häiringute tõttu ei pruugi mõnel juhul mõõdetud andmed „öigemad” olla kui modelleeritud. Üldiselt olid järelarvutuse tuule kiiruse ja suuna tulemused heas kooskõlas vaatlusandmetega (joonis 4). Parim kokkulangevus oli Kihnu ning probleemseim oli see Vilsandil, kus sektoris  $210\text{--}250^\circ$  on teadaolevalt tuule kiirust oluliselt kahandatud mõõtemasti läheduses paiknevate hoonete ja tuletorni tõttu (Jaagus & Kull, 2011). Samuti võisisid erinevused mõõtmiste ja modelleerimistulemuste vahel pärineda WRF-i topograafia ja võrgu horisontaalse lahutuse iseärasustest, millest tulenevalt oli keeruline saada kõrglahutusega andmeid. Lisaks on rasteriseeritud atmosfäärimudeli arvutatud tuul üldjuhul (ka teiste sarnaste mudelite puhul) pisut liiga sujuv (silutud), mis ei arvesta hästi maa-mere piirialal esinevate väikeste lokaalsete eripäradega.

Veetaseme järelarvutus (*hindcast*, „lähteolukord”, joonis 5) 2005.a Gudruni tormi tipphetkel näitas meretõusu e ajuvee (*storm surge*) koondumist Pärnu lahe pärasse. Simuleeritud veetõus Pärnu jõe suudmes oli heas vastavuses vaatlusandmetega, kus tormitõusu esimese tipu kõrguse erinevus oli vaid 6 cm (joonis 6). Seega olid tuleväljad ilmselt piisavalt hästi simuleeritud (joonis 4). FVCOM reprodutseeris kaks veetaseme maksimumi, kus teise tipu esinemise põhjus ei sisaldu tuleväljas, vaid pigem Liivi lahe okeanograafias. Ilmselt aitas sekundaarsele tipule kaasa Liivi lahe 5-tunnine omavõnke- ehk seišiperiood (Suursaar jt., 2003). See teine tipp oli aga mudeli poolt pisut ülehinnatud. Suurima erinevusena torkab siiski silma järelarvutuse („lähteolukord”; joonis 6) tormisündmuse pikem kestus: veetase ei langenud nii kiresti kui tegelikud mõõtmistulemused näitasid. See omakorda oli arvatavasti põhjustatud modelleeritud tuulesündmuse pikemast kestusest ja suuremast „silutusest” (joonis 4).

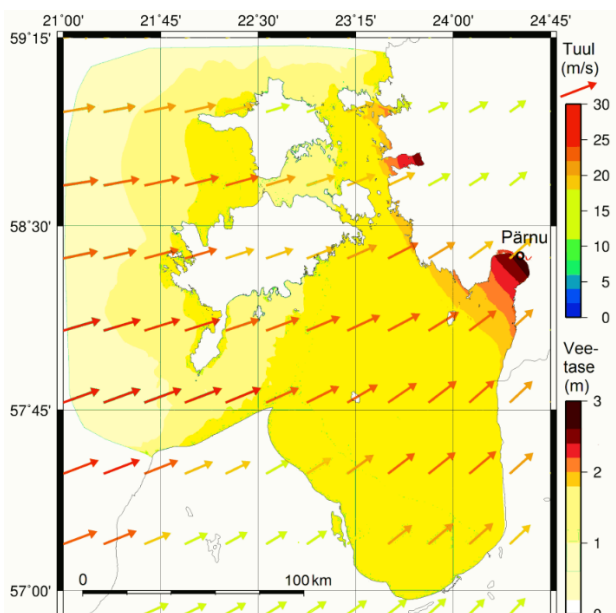


**Joonis 4.** Simuleeritud ja mõõdetud tuule võrdlus Gudruni ajal kuues vaatlusjaamas.

**Figure 4.** Wind speed and direction comparison between observations and simulations in six meteorological stations.

#### 4. Tulevikutormi simulatsioonid

Tehes meremudeli arvutused uute, „tuleviku Gudruni” sisaldavate atmosfääriväljadega, selgus, et ükski tulevikusimulatsiooni stsenaarium (joonis 6: RCP4.5, RCP8.5; aastad 2050 ja 2100) ei muutnud vaadeldud tormi järelarvutatud lähteolukorras tugevamaks. Meie tulemustest nähtub, et näitena arvutatud ekstreemse tulevikutormi intensiivsus ja vastav tormitõus jäi umbes samaks või hoopiski pisut vähenes. Tuleb aga silmas pidada, et tegemist on üksiksündmuse arvutusega ja tulevikku puudutavaks klimatoloogiliseks üldistuseks oleks vaja läbi arvutada rohkem tormisündmusi, sealhulgas erinevatel aastaaegadel (kuudel) toimuvaid ning erinevaid trajektoore pidi kulgevaid torme. Leitud tulemus on näilises vastuolus levinud (ja intuitiivselt eeldatava) seisukohaga, kus kliima globaalne soojenemine toob automaatselt kaasa tormisuse tõusu. Tormisust käsitlevad tulevikutsenaariumid erinevad siiski laiades piirides sõltuvalt piirkonnast, mudelitest, algandmetest (Ulbrich jt., 2009). Arvatavasti esineb ka meie mudelites (nagu teisteski) puudusi ning arvessevõtmata seoseid; ühtegi mudelite ei saa tuleviku suhtes pidada tõsikindlaks enne, kui tulemus pole valideeritud.

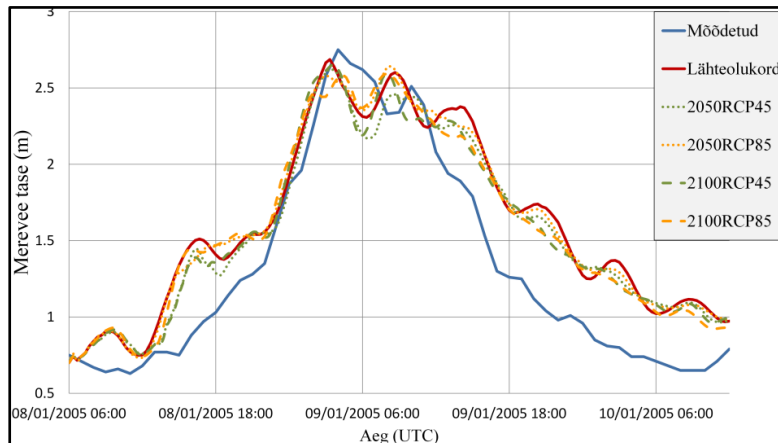


**Joonis 5.** Modelleeritud tuulevälgi ja meretase ajuvee tipphetkel (269/275 cm modelleeritud/mõõdetud Pärnus; aeg 03:20 UTC 9. jaanuar 2005).

**Figure 5.** Modelled wind field and sea level in the storm surge peak (269/275 cm modelled/measured at Pärnu at 02:00 UTC in 9th of January 2005).

Kui püüda tõlgendada meie saadud ühe tulevikutormi arvutustulemust, siis peamiseks tormi mittetugevnemise põhjuseks võib pidada parasvöötme tsüklonite arengu eripära. Nimelt, sellised tsüklonid ammutavad oma energia polaarfrondilt, kus puhuvad kokku külm ja suhteliselt soojem õhumass. Kui tropilised tsüklonid ammutavad energia ookeani pinnasoojusest ja niiskusest, muutudes merepinna temperatuuri tõustes tugevamaks (Tasnim jt., 2015), siis väljaspool tropikat kujunenud tsüklonite intensiivsuse põhilised mõjutajad (mudelis kasutatud parameetrite juures) on tõenäoliselt õhutemperatuuri erinevused frondi piirkonnas. Väiksem temperatuuride erinevus polaarfrondil tulevikus viibki nõrgemate tormide kujunemiseni. Toodud tulevikutsenaarium ei pruugi aga realiseeruda. Peale praegu kõige tõenäolisemaks peetavate ansamblikeskmiste eksisteerib ka äärmuslikumaid tulevikutsenaariume. Näiteks leiavad Hansen jt. (2016), et Gröönimaa jäälkilbi sulamisega võib kaasneda Põhja-Atlandi ookeani tsirkulatsiooniskeemi oluline muutumine, mis kutsub esile muu hulgas ka tugevamad mittetroopilised tormid (supertormid).

Selleks et saada täpsemaid tulemusi tuleviku simulatsioonide kohta lokaalsel (Pärnu) tasandil, oleks vaja uurimistöös kasutatud metoodikat edasi arendada, arvestada 1) glatsio-isostaatilise maakerke ja merepinna tõusu vahekorda tulevikus; 2) laiendada ookeanimudelis kõrgresolutsiooniga maapinna kõrgusandmete ja rannikumere sügavusandmetega kaetud ala; 3) arvestada ka Pärnu jõe vooluhulka ning sademeid, sest parasvöötme tsükloniid võivad tulevikus rohkem niiskust pooluse suunas kanda; 4) kasutada kõrgema resolutsiooniga atmosfääri järelanalüüs (ERA-Interim) andmeid; 5) kasutada ansamblilihenemist, kaasates mitmeid CMIP5 globaalseid kliimamudeleid; 6) arvutada läbi erinevate trajektooridega ja eri aastaaegadel asetleidvaid torme.



**Joonis 6.** Pärnu mõõdetud ja simuleeritud mereveetasemete võrdlus.

**Figure 6.** Storm surge height comparison between all the cases at Pärnu.

## 5. Kokkuvõte

Atmosfääri-mere mudelisüsteemi järelarvutuse tulemused 2005. a tormi Gudruni jaoks olid Lääne-Eestis heas kooskõlas reaalsete vaatlusandmetega. Manipuleeritud atmosfääriandmetega arvutatud tulevikutormi („tuleviku Gudruni“) simulatsioon meie kasutatud metoodika juures ei näidanud tormi intensiivsuse kasvu, vaid tugevuse umbkaudu samasugust taset või isegi mõningast langust. Selle nähtuse põhjuseks võib hüpoteesina pakkuda, et kui troopilised tsükloniid muutuvad merepinna temperatuuri tõustes tugevamaks, siis väiksem temperatuuride erinevus polaarfrondil võib tulevikus viia nõrgemate tormide kujunemiseni parasvöötmes. Sellise üldistuse kontrollimiseks on tulevikus vaja läbi arvutada suurem hulk erinevates tingimustes kulgevaid tormisündmusi.

## 6. Tänuavaldused

Seda uurimust on toetanud Eesti teadusagentuuri personaalse uurimistoetuse projekt PUT595 ja Jaapani haritusministeeriumi grant nr 22404011 (Waseda Ülikool).

## 7. Kirjanduse viited

- Avotniece, Z., Rodinov, V., Lizuma, L., Briede, A., Kļaviņš, M., 2010. Trends in the frequency of extreme climate events in Latvia. *Baltica*, 23 (2), 135–148.
- Berz, G., Conrad, K., 1994. Stormy weather: the mounting windstorm risk and consequences for insurance industry. *Ecodecision*, 12, 65–69.
- Chen, C., Liu, H., Beardsley, R.C., 2003. An Unstructured Grid, Finite-Volume, Three-Dimensional, Primitive Equations Ocean Model: Application to Coastal Ocean and Estuaries. *J. Atmos. Ocean Technol.*, 20 (1), 159–186.
- Christensen, O.B., Kjellström, E., and Zorita, E., 2015. Projected change – atmosphere. In: The BACC II Author Team. *Second Assessment of Climate Change for the Baltic Sea Basin*. Cham: Springer, pp. 217–233.
- Eelsalu, M., Soomere, T., Pindsoo, K., Lagemaa, P., 2014. Ensemble approach for projections of return periods of extreme water levels in Estonian waters. *Continental Shelf Research*, 91, 201–210.
- Emanuel, K., 2005. Increasing destructiveness of tropical cyclones over the past 30 years. *Nature*, 436, 686–688.

- Feser, F., Barcikowska, M., Krueger, O., Schenk, F., Weisse, R., Xia, L., 2015. Storminess over the North Atlantic and northwestern Europe – A review. *Quarterly Journal of the Royal Meteorological Society*, 141 (687), 350–382.
- Hansen, J., Sato, M., Hearty, P., Ruedy, R., Kelley, M., Masson-Delmotte, V., Russell, G., Tselioudis, G., Cao, J., Rignot, E., Velicogna, I., Tormey, B., Donovan, B., Kandiano, E., von Schuckmann, K., Kharecha, P., Legrande, A.N., Bauer, M., Lo, K.-W., 2016. Ice melt, sea level rise and superstorms: evidence from paleoclimate data, climate modeling, and modern observations that 2°C global warming could be dangerous. *Atmos. Chem. Phys.*, 16, 3761–3812.
- Hill, D., 2012. The lessons of Katrina, learned and unlearned. *Journal of Coastal Research*, 29, 324–331.
- Jaagus, J., Kull, A., 2011. Changes in surface wind directions in Estonia during 1966–2008 and their relationships with large-scale atmospheric circulation. *Estonian Journal of Earth Sciences*, 60 (4), 220–231.
- Jaagus, J., Suursaar, Ü., 2013. Long-term storminess and sea level variations on the Estonian coast of the Baltic Sea in relation to large-scale atmospheric circulation. *Estonian Journal of Earth Sciences*, 62, 73–92.
- Knutson, T.R., Tuleya, R.E., 2004. Impact of CO<sub>2</sub>-induced warming on simulated hurricane intensity and precipitation: Sensitivity to the choice of climate model and convective parameterization. *Journal of Climate*, 17 (18), 3477–3495.
- Leckebusch, G.C., Ulbrich, U., 2004. On the relationship between cyclones and extreme windstorm events over Europe under climate change. *Global and Planetary Change*, 44 (1-4), 181–193.
- Nakamura, R., Iwamoto, T., Shibayama, T., Mikami, T., Matsuba, S., Mäll, M., Takekouji, A., Tanokura, Y., 2015. Field survey and mechanism of storm surge generation invoked by the low pressure with rapid development in Nemuro Hokkaido in December 2014. *Journal of Japan Society of Civil Engineers*, 71, 31–36.
- Nakamura, R., Shibayama, T., Esteban, M., Iwamoto, T., 2016. Future typhoon and storm surges under different global warming scenarios: case study of typhoon Haiyan (2013). *Natural Hazards*, 1–37.
- Orviku, K., Jaagus, J., Kont, A., Ratas, U., Rivils, R., 2003. Increasing activity of coastal processes associated with climate change in Estonia. *Journal of Coastal Research*, 19 (2), 364–375.
- Post, P., Kõuts, T., 2014. Characteristics of cyclones causing extreme sea levels in the northern Baltic Sea. *Oceanologia*, 56(S), 241–258.
- Roberts, J.F., Champion, A.J., Dawkins, L.C., Hodges, K.I., Shaffrey, L.C., Stephenson, D.B., Stringer, M.A., Thornton, H.E., Youngman, B.D., 2014. The XWS open access catalogue of extreme European windstorms from 1979 to 2012. *Natural Hazards and Earth System Sciences*, 14 (9), 2487–2501.
- Rutgersson, A., Jaagus, J., Schenk, F., Stendel, M., Bärring, L., Briede, A., Claremar, B., Hanssen-Bauer, I., Holopainen, J., Moberg, A., Nordli, Ø., Rimkus, E., Wibig, J., 2015. Recent change – atmosphere. In: The BACC II Author Team (Ed.). *Second Assessment of Climate Change for the Baltic Sea Basin*, pp. 69–97. Springer.
- Schmidt, H., von Storch, H., 1993. German Bight storms analysed. *Nature* 370 : 791
- Shibayama, T., 2015. Field surveys of recent storm surge disasters. *Procedia Engineering*, 116, 179–186.
- Skamarock, W.C., Klemp, J.B., Dudhia, J., Gill, D.O., Barker, D.M., Duda, M.G., Huang, X.Y., Wang, W., Powers, J.G., 2008. A Description of the Advanced Research WRF Version 3, NCAR Technical Note.
- Suursaar, Ü., Jaagus, J., Tõnnisson, H., 2015. How to quantify long-term changes in coastal sea storminess? *Estuarine Coastal and Shelf Science*, 156, 31–41.
- Suursaar, Ü., Kullas, T., Otsmann, M., Kõuts, T., 2003. Extreme sea level events in the coastal waters of western Estonia. *Journal of Sea Research*, 49, 295–303.
- Suursaar, Ü., Kullas, T., Otsmann, M., Saaremäe, I., Kuik, J., Merilain, M., 2006. Hurricane Gudrun and modelling its hydrodynamic consequences in the Estonian coastal waters. *Boreal Environment Research*, 11, 143–159.
- Tasnim, K.M., Shibayama, T., Esteban, M., Takagi, H., Ohira, K., Nakamura, R., 2015. Field observation and numerical simulation of past and future storm surges in the Bay of Bengal: case study of cyclone Nargis. *Natural Hazards*, 75 (2), 1619–1647.
- Trenberth, K., 2005. Uncertainty in hurricanes and global warming. *Science*, 308, 1753–1754.
- Tõnnisson, H., Orviku, K., Jaagus, J., Suursaar, Ü., Kont, A., Rivils, R., 2008. Coastal damages on Saaremaa Island, Estonia, caused by the extreme storm and flooding on January 9, 2005. *Journal of Coastal Research*, 24 (3), 602–614.
- Ulbrich, U., Leckebusch, G.C., G. Pinto, J. G., 2009: Extra-tropical cyclones in the present and future climate: A review. *Theor. Appl. Climatol.*, 96, 117–131.
- Watanabe, M., Suzuki, T., O’ishi, R., Komuro, Y., Watanabe, S., Emori, S., Takemura, T., Chikira, M., Ogura, T., Sekiguchi, M., Takata, K., Yamazaki, D., Yokohata, T., Nozawa, T., Hasumi, H., Tatebe, H., Kimoto, M., 2010. Improved Climate Simulation by MIROC5: Mean States, Variability, and Climate Sensitivity. *J. Climate*, 23, 6312–6335.

Webersik, C., Esteban, M., Shibayama, T., 2010. The economic impact of future increase in tropical cyclones in Japan. *Natural Hazards*, 55 (2), 233–250.

## **Modelling storm surge conditions under future climate scenarios: A case study of 2005 January storm Gudrun in Pärnu, Estonia**

Martin Mäll

*University of Tartu, Institute of Ecology and Earth Sciences*

Ryota Nakamura, Tomoya Shibayama

*Department of Civil and Environmental Engineering, Waseda University, Japan*

Ülo Suursaar

*University of Tartu, Estonian Marine Institute*

Ain Kull

*University of Tartu, Institute of Ecology and Earth Sciences*

### **Summary**

A case study based on the January 2005 storm Gudrun parameters has shown good agreement between observations and results obtained from atmospheric and ocean models. In methodology used by us for simulating „future storm Gudrun“ no increase in the intensity of this particular future storm was found, but instead a slight decrease was noticed. When tropical cyclones get stronger with higher sea surface temperatures then for extratropical cyclones this does not apply. Instead, smaller air temperature differences in the polar front may lead to weaker extratropical cyclone formation. However, for drawing broader conclusions, a number of different storm cases should be simulated.

# MODELLING A STORM SURGE UNDER FUTURE CLIMATE SCENARIOS: CASE STUDY OF STORM GUDRUN

Martin Mäll, University of Tartu, [martin.mall@ut.ee](mailto:martin.mall@ut.ee)

Ryota Nakamura, Waseda University, [shibayama@waseda.jp](mailto:shibayama@waseda.jp)

Tomoya Shibayama, Waseda University, [ryota\\_nakamura617@yahoo.co.jp](mailto:ryota_nakamura617@yahoo.co.jp)

Ülo Suurhaar, University of Tartu, [ulo.suurhaar@ut.ee](mailto:ulo.suurhaar@ut.ee)

Ain Kull, University of Tartu, [ain.kull@ut.ee](mailto:ain.kull@ut.ee)

## INTRODUCTION

The most dangerous natural hazards in the Baltic Sea region are related to extra-tropical cyclones (ETC). This practically tideless region lies near the North-Atlantic storm track where, during the colder half of the year, storms from west-southwest occur, building up to temporal Baltic Sea level rise and additional site-dependent storm surge. On January 9th 2005, the storm called Gudrun caused a record high surge in Pärnu city at +275 cm above the mean sea level. It became the most influential natural disaster in Estonia. The aim of this study is (1) to reconstruct the historical storm surge event using the Weather Research and Forecasting (WRF-ARW) model and Finite Volume Community Ocean Model (FVCOM), and (2) by modifying the background forcing conditions in accordance with the IPCC AR5 proposed climate change scenarios RCP4.5 and RCP8.5 for 2050 and 2100, to simulate the “future Gudrun” extreme surge (see e.g. Tasnim et al. 2015).

## METHODS

Top-down approach was adapted where atmospheric model is run first with NCEP FNL Operational Global Analysis data and the output is used as an input for the ocean model in order to simulate the storm surge (base case). Three nested domains were used in WRF. Domain one runtime was 96 hours and domain three was 54 h. Future simulations were run under CMIP5 model MIROC5 data forcing for sea surface temperature (SST), air temperature and relative humidity. Each RCP scenario was run under the years 2050 and 2100 where the mean values of parameters were obtained from the 2045-2055 and 2091-2100, respectively.

## RESULTS

Hindcast results for wind speed and direction were in good agreement with the observations. A few smaller differences appeared due to limited resolution of the WRF model; also gridded model winds are usually quite smooth which cannot take into account small-scale local features especially on the land-sea interface. The simulated storm surge height was in good agreement with observations, where the peak difference was 7 cm (Fig. 1,2). The FVCOM was competent in simulating two peaks as it was observed. However, the second peak, (generated by the Gulf of Riga seiche period) was moderately overestimated. Due to the complexity of the western Estonia's coastline, even slight deviation of the cyclone track can have a noticeable impact to simulation results at a specific location. It appeared that storm surge intensity did not increase under any future simulations. In fact, a decrease was noted for both RCP4.5 cases whereas no significant change was observed for RCP8.5 cases.

Probably the main reasoning behind the lack of increase lies in the mechanisms of ETC-s. Such cyclones harvest their energy along the polar front where cold and warm air masses interact, whereas tropical cyclones derive energy from SST. Differently from the tropical cyclones, SST rise did not cause ETC-s intensification. As the difference in atmospheric air temperatures between poles and tropics decrease, the energy absorbed by the ETC-s decreases and therefore possibly leads to weaker storms in the mid-latitudes zone of westerlies.

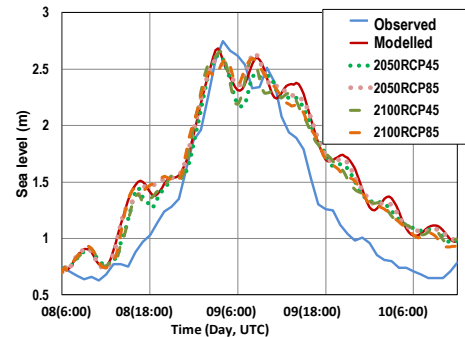


Figure 1 - Comparison of different scenario simulations using 2005 January storm surge conditions at Pärnu.

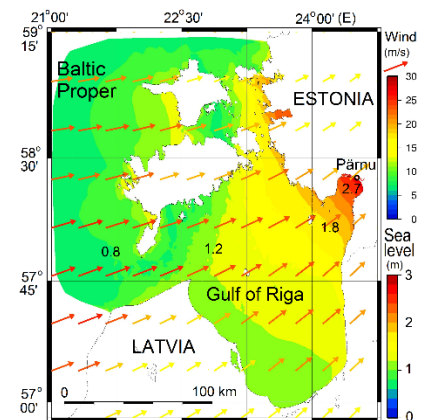


Figure 2 - Spatial variations of the storm surge sea level.

## REFERENCES

- Tasnim, Shibayama, Esteban, Takagi, Ohira, Nakamura (2015): Field observation and numerical simulation of past and future storm surges in the Bay of Bengal: case study of cyclone Nargis. Natural Hazards, 75: pp. 1619-1647.

# 2014年12月に北海道で発生した温帯低気圧による根室の高潮被害の現地調査と発生機構の解明

中村 亮太<sup>1</sup>・岩本 拓夢<sup>1</sup>・柴山 知也<sup>2</sup>・三上 貴仁<sup>3</sup>・  
松葉 俊哉<sup>4</sup>・Martin MAELL<sup>5</sup>・館小路 晃史<sup>1</sup>・田野倉 祐介<sup>6</sup>

<sup>1</sup> 学生会員 早稲田大学大学院 創造理工学研究科（〒169-8555 東京都新宿区大久保3-4-1）  
E-mail: ryota\_nakamura617@yahoo.co.jp

<sup>2</sup> フェロー会員 早稲田大学教授 工学院（〒169-8555 東京都新宿区大久保3-4-1）

<sup>3</sup> 正会員 早稲田大学講師 工学院（〒169-8555 東京都新宿区大久保3-4-1）

<sup>4</sup> 国土交通省 東北地方整備局北上川下流事務所（〒986-0861 宮城県石巻市蛇田新下沼80）

<sup>5</sup> 早稲田大学大学院 創造理工学研究科（〒169-8555 東京都新宿区大久保3-4-1）

<sup>6</sup> 東京工業大学大学院 情報理工学研究科情報環境学専攻（〒152-8550 東京都目黒区大岡山2丁目12-1）

2014年12月中旬に発生した温帯低気圧は急速に発達し、根室に高潮被害をもたらした。本研究では、根室に生じた高潮の現地調査の結果を整理し、数値モデルを用いて高潮の再現を試みた。現地調査の結果、根室市街地の浸水高は最大で2.20mであった。一方、根室港では最大の2.82mを記録した。現地調査の結果、地盤高が海岸線から市街地に向けて徐々に低下していた。この地形的特性が根室市弥生町市街地に高潮被害をもたらした原因の一つである。数値計算の結果、根室湾で水位が上昇・下降する現象が見られた。具体的には、まず東風が吹き、根室湾の水位が上昇する。次に、風向きが北風に変化して、根室湾に溜まった水塊が根室半島に吹き寄せられ、根室港での高潮偏差が増加するという結果を得た。根室市街地の地形的特性、風向きの変化と根室湾と根室半島の相対的位置関係などの条件が高潮被害をもたらした。

**Key Words :** low pressure system, storm surge, field survey, Nemuro ,inundation, WRF, FVCOM

## 1. 序論

近年、世界各地で台風による高潮被害が頻発している。例示すれば、2013年に発生した台風Haiyan<sup>1)</sup>は、フィリピンのレイテ島一帯に高潮被害をもたらした。また、地球温暖化に伴う台風の強化により高潮被害の増加も予測されている<sup>1)</sup>。そこで、台風による高潮災害を詳細に算定可能な気象・海洋数値モデルの検証が行われてきた(例えば、吉野ら<sup>2)</sup>)。一方で、急速発達する温帯低気圧に伴う海洋現象の研究では、森ら<sup>3)</sup>による暴風浪特性に関する研究が行われているが、高潮の研究例は少ない。これは、急速発達する低気圧による高潮の被災件数が過去に例が少ないと考えられる。そのため、急速発達する低気圧による高潮という特別な事例を詳細に分析し、災害素因を評価することは、沿岸付近の防災力向上に必要であると考えた。

2014年12月16日から17日にかけて急速に発達した低気圧は、根室港および根室の市街地に高潮被害をもたらした。2014年から2015年の冬季は、中心気圧が980hPaを下回る低気圧が北海道の付近を通過するという気象現象が例年より多く見受けられた<sup>4)</sup>。今後もこの傾向が継続する場合には、同様の発生機構を有した高潮が生じる可

能性が高まると考えられる。

本論文では、①発生した低気圧の特性の分析、②高潮被災の現地調査、③数値モデルによる検討、の3段階の検証を行い、根室に高潮を引き起こした低気圧及び高潮の物理特性を解明し、高潮の発生機構の評価を試みる。

## 2. 2014年12月に発生した低気圧の特性

2014年12月16日12時に日本海中部と四国の南部の海面正気圧が992 hPaと1002 hPaの低気圧は、ともに北東に進み、17日の9時に北海道東部の海上で948hPaの勢力をもつ低気圧へと急速発達した<sup>5),6)</sup>。最大風速は、根室市納沙布で30.7 m/s、最大瞬間風速は、根室市弥栄町で39.9 m/sであった<sup>5)</sup>。根室では、低気圧の接近により、17日午前に潮位がTP+1.7~1.9 mとなった<sup>7)</sup>。これにより、高潮による住居の床上・床下浸水が発生した<sup>5)</sup>。

図-1は、12月17日9時の気象庁速報天気図である<sup>6)</sup>。急速発達した低気圧が北海道東部海上に存在している。また、図-2の12月18日6時の気象庁速報天気図<sup>6)</sup>をみると、発達した低気圧は約1日間、北海道の東部海上に留まっていた。中心気圧の値は、日本に襲来する台風と同程度で

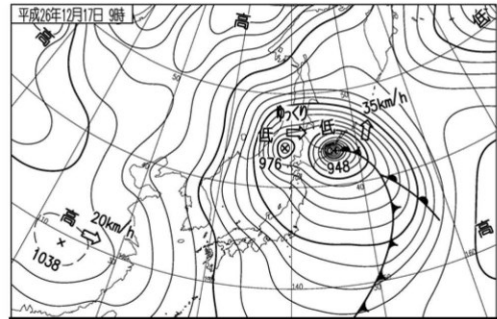


図-1 気象庁速報天気図の一部抜粋<sup>⑥)</sup>

(12月17日の午前9時)

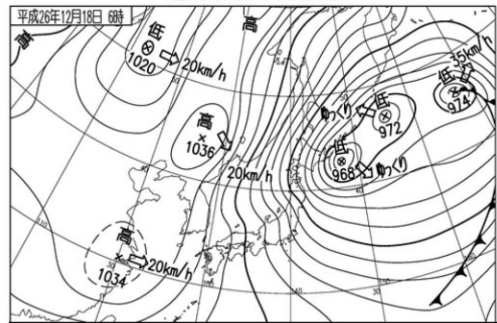


図-2 気象庁速報天気図の一部抜粋<sup>⑥)</sup>

(12月18日の午前6時)

あり、台風の勢力と同等の勢力をこの温帯低気圧は有していたといえる。更に、等圧線が台風の等圧線のように同心円に近いという特性も有していた（図-1）。

### 3. 現地調査結果

現地調査は2014年12月19日に実施した。高潮発生2日後であるため、高潮浸水の痕跡がはっきりと残っていた。表-1に高潮痕跡高の諸情報を示す。11地点で調査を行った。ここで、浸水高は高潮来襲時の天文潮位からの痕跡高であり、遡上高は海岸から内陸へ高潮が駆け上がる際の到達点の高さである。本論文では、17日午前9時の天文潮位を使用している。図-3は、根室市弥生町市街地の測定点の分布である。市街地での最大浸水高は、地点Dの2.20 mであった。海岸線から弥生町交差点の付近にかけて、地盤高が低下している（表-1）。海岸線の地盤高を高潮が超えると内陸に浸水しやすい地形をしていたことを示している。弥生町交差点付近の地形特性も高潮浸水域が拡大した一因である。図-4は根室港付近の測定点の位置である。根室港では、市街地と比較して浸水高が全体的に高かった。根室港では、地点Kで1.80 mを計測し、より湾奥の地点Jでは、2.82 mを記録した。この現地調



図-3 根室市弥生町交差点付近の測定位置

(Google Earth に加筆)



図-4 根室港付近の測定位置

(Google Earth に加筆)

査の結果から、港湾のような狭い範囲内でも、港奥は高潮が高くなっていた。港奥では、急に水深が減少しており、なおかつ港奥は境界があり水が溜まりやすいため、港奥での高潮偏差が上昇したと考えらえる。2.80mの浸水高さを記録した根室港にある地点Jにおいても、家屋の破壊は見られなかった。今回の低気圧によって引き起こされた高潮は、2013年にフィリピンで発生した高潮と異なり、段波を伴わない、徐々に海面が上昇する高潮であつたため、高潮前面での衝撃波圧が大きくななく、構造物に物理的な被害を及ぼさなかつたと考えられる。

表-1 高潮痕跡高（地盤高はTP+ 表示）

測定地点	緯度	経度	地盤高(m)	高さ(m)	種別	根拠
A	43°19'57.90"	145°34'42.54"	TP+ 0.83	1.66	浸水高	痕跡
B	43°19'57.90"	145°34'42.54"	TP+ 0.83	1.59	浸水高	痕跡
C	43°19'57.90"	145°34'42.54"	TP+ 0.83	1.56	浸水高	痕跡
D	43°19'58.26"	145°34'43.32"	TP+ 1.24	2.20	浸水高	住民の証言
E	43°19'58.27"	145°34'41.45"	TP+ 0.70	1.39	浸水高	痕跡
F	43°19'57.06"	145°34'43.58"	TP+ 1.71	1.41	遡上高	雪が溶けている
G	43°20'00.94"	145°34'45.41"	TP+ 1.84	2.16	浸水高	住民の証言
H	43°19'58.30"	145°34'46.95"	TP+ 1.52	1.74	浸水高	住民の証言
I	43°19'58.10"	145°34'47.40"	TP+ 1.47	1.55	浸水高	住民の証言
J	43°20'21.72"	145°35'06.78"	TP+ 2.07	2.82	浸水高	住民による写真
K	43°20'38.16"	145°35'06.78"	TP+ 1.89	1.80	浸水高	住民による写真
標高1	43°20'01.69"	145°34'37.82"	TP+ 1.56	-	地盤高	-
標高2	43°20'00.84"	145°34'38.10"	TP+ 1.40	-	地盤高	-
標高3	43°19'59.76"	145°34'39.42"	TP+ 1.20	-	地盤高	-
標高4	43°19'58.20"	145°34'41.40"	TP+ 0.79	-	地盤高	-

表-2 計算条件の設定

項目	内容
計算期間 (fnl-1, gfs-1)	2014年12月16日21:00 - 2014年12月18日 03:00 (JST)
計算期間 (fnl-2, gfs-2)	2014年12月17日03:00 - 2014年12月18日 03:00 (JST)
W R F W R F TC ボ ガス F V C O M	ドメイン1 (grids, range, mesh) 120×120, WE: 133.8° -152.2° , SN: 34.8° - 48.5° , 15 km ドメイン2 (grids, range, mesh) 201×221, WE: 142.9° -149.1° , SN: 41.0° - 46.0° , 3 km 鉛直層及び頂点気圧 36 layers and 2000 Pa 雲微物理スキーム WSM 6 <sup>14)</sup> 積雲対流スキーム Kain-Fritsch <sup>15)</sup> 投影法 Mercator 埋め込み期間 2014年12月16日21:00 - 2014年12月18日 03:00 (JST) ドメイン (grids, range, mesh) 400×400, EW: 137.8° -150.2° , SN: 34.9° - 46.6° , 3 km 鉛直層及び頂点気圧 36 layers and 2000 Pa 最大風速半径 50km, 60km, 70km, 80km, 90km, 100km 計算時間 各ケースのWRFの計算時間と同一 計算範囲 EW: 144.2° -146.7° , SN: 42.3° - 45.1° Cell 114782 Node 58594 σ vertical layer 11



図-5 根室周辺における非構造格子の地形の一部

#### 4. 算定手法の概要

算定手法は、中村ら<sup>8)</sup>が台風 Yolanda (2013) に使用した手法と同様に、気象モデルには ARW-WRF<sup>9)</sup>を使用し、海洋モデルには FVCOM<sup>10)</sup>を使用した。各モデルの詳細な計算条件の設定を表-2 に示す。

##### 1) 気象モデルの WRF の設定

本研究では、WRF に FNL<sup>11)</sup>、GFS<sup>12)</sup>を用いた標準的な手法と TC ボーガス<sup>13)</sup>を WRF の計算結果として逐次的に埋め込み、気象場を決定した手法を用いて、低気圧を再現した。FNL と GFS の初期気象場が計算結果に与える影響を考慮して、開始時間を 2 ケース設定した。FNL を用いた、計算開始時間が 16 日 21 時、17 日 3 時のケース名をそれぞれ、fnl-1, fnl-2 とした。GFS を用いたケース名も同様に設定した。TC ボーガスを用いたケースでは、最大風速半径を 60, 70, 80, 90, 100 km と設定した。ケース名は、先頭に TC と最大風速半径の値で示している。以上の合計 9 ケースの計算を行った。TC ボーガスは、同心円形の気象場を再構成する手法である。発生した低気圧の中心付近の海面更正気圧が同心円状に広がっていたことを考慮すると、発生した低気圧は台風の形状に近い。気圧分布の対称性という観点からは TC ボーガスの利用も許容できると考えた。TC ボーガスを用いた計算は、気象庁が発表した速報天気図から海面更正気圧とその中心位置を決定し、Atkinson・Holliday<sup>16)</sup>が提案した以下の式 (1) を用いて、最大風速を決定した。

$$V_m = 3.45(1010 - MSLP)^{0.644} \quad (1)$$

ここに、 $V_m$  : 最大風速 (m/s),  $MSLP$  : 最低海面更正気圧 (hPa) である。

##### 2) 海洋モデルの FVCOM の設定

海面抵抗係数に本多・光易の式<sup>17)</sup>に横田ら<sup>18)</sup>の風速 30 m/s 以上は一定となるとの条件を加えた式 (2) を用いた。

$$\begin{aligned} C_D &= (1 - 0.01890 \times W_s) \times 0.00128 \quad (W_s \leq 8 \text{ m/s}) \\ C_D &= (1 + 0.1078 \times W_s) \times 0.000581 \quad (8 \text{ m/s} \leq W_s \leq 30 \text{ m/s}) \\ C_D &= 0.00246 \quad (W_s \geq 30 \text{ m/s}) \end{aligned} \quad (2)$$

ここに、 $C_D$  : 海面抵抗係数、 $W_s$  : 風速 (m/s) である。

海底地形には GEBCO\_08<sup>19)</sup>を使用した。海岸線は SRTM 90 m<sup>20)</sup>を使用した。図-5 は、FVCOM で使用した非構造格子の地形の一部である。根室付近の最小の格子幅は約 100 m と設定した。非構造格子を使用すると根室半島の複雑な地形に沿った海岸線を作成できる (図-5)。

#### 5. 算定結果と考察

##### 1) 気象モデルの計算結果

###### a) 根室市弥栄町における風速の比較

図-6 は、弥栄町における風速の算定結果と観測値の比較である。17 日 5 時と 9 時に風速の観測値は 25 m/s を超えている。ここで、FNL と GFS の各ケースの風速計算結果は、観測値とよく一致している。特に、17 日 5 時から 9 時における風速の急激な変化を算定している。一方で、TC ボーガスのケースでは、低気圧の中心が根室を通っていないため、風速の急激な変化を算定していないが、TC-60 の全体的な風速値は観測値に近かった。最大風速半径を増大させると観測値との差異も増加した。

###### b) 根室市弥栄町における風向の比較

表-3 では、弥栄町における計算結果と観測値の風向を比較している (紙面の都合上、各ケースの平均風向を掲載)。FNL と GFS の各ケースでは、午前 8 時以降には西南西の風に変化しており、観測値の風向と合致していない。一方で、TC ボーガスを用いた場合の風向は午前 8 時、9 時は、北北西、北西であり、観測値と比較して若干の差異はあるものの、よく一致している。

###### c) 根室市弥栄町における海面更正気圧の比較

図-7 は、弥栄町における、海面更正気圧の算定値と観測値である。観測値は、17 日 8 時に 950 hPa まで低下している。この時間には温帯低気圧の中心気圧が 948 hPa

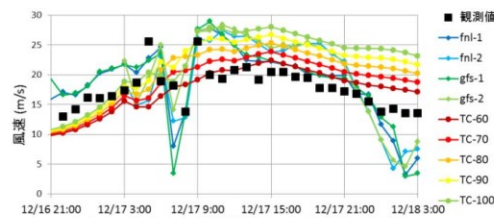


図-6 根室市の観測所における風速の比較

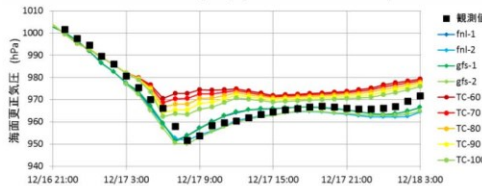


図-7 根室市の観測所における海面更正気圧の比較

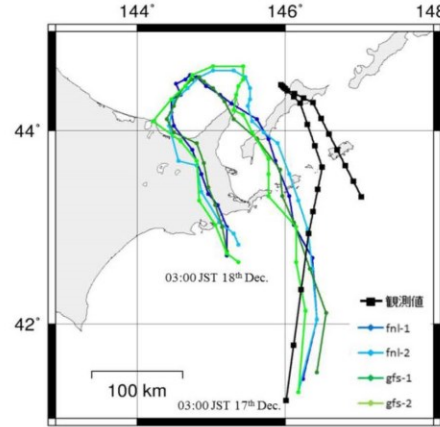


図-8 低気圧の中心位置の比較

表-3 根室市の観測所における風向の比較											
	2014/12/17	3:00	4:00	5:00	6:00	7:00	8:00	9:00	10:00	11:00	12:00
観測値	東	東	東	北北東	北北東	北	西北西	西	西南西	西南西	
FNLとGFSの平均値	東	東	東北東	北東	西南西	西南西	西南西	西南西	西南西	西南西	
TCケースの平均値	東	東	東北東	北北東	北	北北西	北西	西北西	西北西	西北西	

であるため、気圧の中心位置を考慮すると、低気圧の 950 hPa 以下の範囲が約 80 km 広がっていた可能性がある。FNL と GFS を用いた 4 ケースは、観測値とよく一致している。これは、根室の上空を低気圧が通過したためである。一方で、TC ボーガスを用いたケースは、最大風速半径が 60 km の場合に、20 hPa 程の差がある。最大風速半径を広げていくにつれて、差異は減少したが、100 km の場合においても 10 hPa 程の差異となっている。

#### d) 低気圧の経路の比較

図-8 は低気圧の中心位置の 17 日午前 3 時以降の 1 時間毎の時間変化である。気象庁の速報値から求めた低気圧の中心を観測値として表示している。TC ボーガスを用いた各ケースは、観測値を基に低気圧を埋め込んでいたため、その経路は気象庁の観測値と同一となる。FNL と GFS を用いて計算した低気圧は、17 日 6 時頃まで観測値の経路とよく一致しているが、観測よりも早い時間に根室付近を通り過ぎている。これが、風向の変化が観測値よりも早い時間に変化した原因である。急速発達する低気圧の詳細な再現は難しく、観測値の経路との差異は高潮の算定精度に影響を及ぼす可能性が高い。

#### e) 各ケースの気象場の評価

FNL と GFS を用いたケースでは、気圧と風速の急速な変化を算定しているが、高潮が発生した午前 8 時から 9 時の風向を精度よく算定していない。これが高潮偏差の算定精度に影響を与える可能性がある。TC ボーガスのケースは、TC ボーガスが低気圧の構造を詳細に再現できず、速報値に誤差があるためと考えられるため、風速の急激な変化と気圧は精度よく算定できておらず、気圧の差異を考えると最大風速半径の厳密な決定は難しいが、風速・風向の全体的な傾向は TC60 が観測値とよく

合致している。更に、低気圧の算定精度を改善するためには、JMA-MSM の使用、低気圧の中心位置の誤差の考慮、TC ボーガスの改良や経験式の使用などの方法が考えられる。これらについては今後の課題としたい。

## 2) 海洋モデルによる高潮の算定結果

図-9 は根室港における高潮偏差の比較である。北海道開発局所管施設の根室における観測値<sup>7)</sup>と計測地点 K, J の値は、天文潮位を除いた高潮偏差へ補正している。

#### a) GFS と FNL を用いたケース

GFS と FNL の 4 ケースでは、最大高潮偏差が 0.5~0.6 m 程度に留まっている。この値は、観測値と 1.2~1.3 m 程の差異がある。計算開始時の水位は観測値と比較して、約 0.4 m (fnl-1, gfs-1), 約 0.6 m (fnl-2, gfs-2) と低い。この差異を考慮しても、GFS と FNL の 4 ケースでは約 0.6 m から 0.9 m 過小評価している。これは、GFS と FNL の 4 ケースにおいて、①高潮が発生した午前 8 時から 9 時の風向を精度よく算定していないため、②根室港では風速値は観測値近いが、根室湾から太平洋側にかけての海上で、低気圧による風速の全体的な強度を過小評価した、という 2 つの理由が考えられる。①については、時

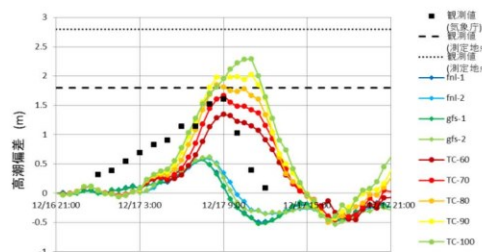


図-9 根室港における高潮偏差の比較

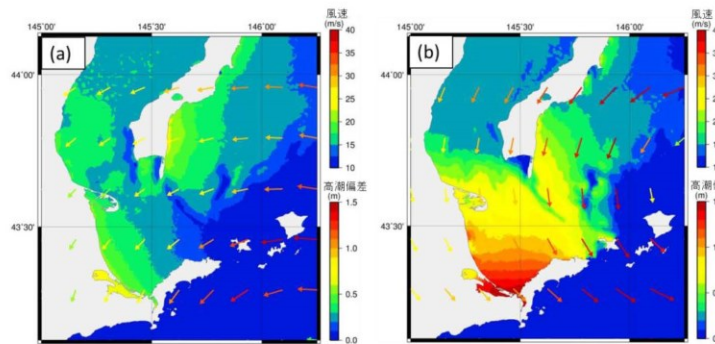


図-10 TC-60 の根室周辺の高潮偏差と風速（矢印の色が風速を示す）(a) 17 日 6 時 00 分, (b) 17 日 9 時 00 分

系列全体の風向の観測値との差異に加えて、最高偏差を観測した 17 日午前 8 時から 9 時における風向が南西よりも変化している。そのため、午前 8 時以降は、根室港の高潮偏差が上昇しきらず、過小評価したと考えられる。実際に、いずれのケースでも午前 7 時に高潮偏差は最高値となっており、上記と符合している。また、FNL, GFS を用いた WRF の計算は、風や気圧を過小評価する傾向があるという報告もあり<sup>8)</sup>、②の理由を裏付けている。

#### b) TC ポーガスを用いたケース

TC ポーガスを用いたケースでは、最大風速半径が 60, 70, 80, 90, 100 km の各ケースで、高潮偏差は 1.3, 1.7, 1.9, 2.0, 2.3 m となっている（図-9）。計算開始時の約 0.4 m の水位上昇を考慮すると、TC-60 の高潮偏差が観測値に近い値となる。これは、風速・風向の算定値と観測値が、面的・時系列的に一致していたためと考えられる（図-6、表-3）。また、気象庁の観測値と比較して、高潮偏差の立ち上がりが遅く、ピーク値のみ観測値と合致している結果になっている。本研究では、高潮算定に波浪の効果を考慮していない。波浪の計算を行い外洋からの波の侵入を考慮することでより詳細に再現できると考えられる。また、午前 9 時以降の急激な風向変化に伴う高潮偏差の急激な減少は、全てのケースで午前 12 時以降となっている。これは、午後 12 時以降に根室の風が西風になったからである。算定された気象場の改善を行うことで、より精度よく高潮を再現することが可能であろう。

#### c) 根室において生じた高潮の発生機構

初期水位の 0.4m を考慮した場合の高潮偏差の傾向と値が最も観測値に近かった TC-60 の高潮偏差の結果を図-10 に示す。図-10 (a) 17 日 6 時と (b) 17 日 9 時の高潮偏差と風速風向を示した図である。図より午前 6 時の時点で高潮偏差の上昇が既に始まっており、午前 9 時には、根室半島周辺北側の海岸線で高潮偏差が上昇している結果となった。まず、東風が吹き、根室湾内の水位が上昇する。次に、低気圧の移動に伴い、徐々に北風に変化して、根室半島の周辺の高潮偏差が上昇し、高潮被害が生じたと考えた。この結果は、時間的な差異はあるが、

TC-60 の風速・風向の観測値との全般的な一致を考慮すると、概ね発生機構を捉えていると考えられる。

## 6. 結論

本研究では、根室市で生じた高潮の現地調査と数値解析の結果を示した。現地調査の結果、被害が生じた地域では、地盤高が海岸から市街地に向かって低下していた。また、数値解析の結果から、まず東風が吹き、根室湾の水位が上昇し、次に、東風が北風に変化して、根室湾に溜まつた水塊が根室半島に吹き寄せて、根室港で高潮偏差が上昇したことが解った。今回の高潮被害は以上のような複数の要因が重なり生じた可能性が指摘できる。根室市街地と根室港は、高潮の影響を受けやすい場所であり、対策が必要である。最後に、低気圧の再現精度をより高めるために、JMA-MSM の使用、TC ポーガス手法の改良や経験式の構築が必要である。また、波浪の効果も検討することで、より詳細に根室で生じた高潮を解明することができる。これらは今後の課題としたい。

**謝辞：**本研究は私立大学戦略的基盤形成支援事業「減災研究の国際展開のための災害研究基盤の形成」、科学研究費補助金基盤(B)No.22404011（ともに、代表者：柴山知也）のもとに行われた。観測当時、早稲田大学社会環境工学科 4 年の金暉氏に現地調査を補佐して頂いた。記して謝意を表する。

## 参考文献

- IPCC : Summary for Policymakers. In: Climate Change 2013: The Physical Science Basis. Contribution of Working Group I to the Fifth Assessment Report of the Intergovernmental Panel on Climate Change [Stocker et al]. Cambridge University Press, Cambridge, United Kingdom and New York, NY, USA. 2013.
- 吉野純、村上智一、林雅典、安田孝志：高潮計算精

- 度に及ぼす入力台風気象場の再現性の影響、海岸工学論文集、Vol.53, pp.1276-1280, 2005.
- 3) 森信人, 高木友典, 川口浩二, 加島寛章, 間瀬肇, 安田誠宏, 島田広昭: 2012年4月3~4日に日本海で急発達した低気圧による暴波浪特性, 土木学会論文集B2 海岸工学, Vol.69, pp.126-130, 2013.
  - 4) 気象庁: 2014/2015 年冬の大気循環場の特徴について, pp.41, [[http://www.data.jma.go.jp/gmd/extreme/kaigi/2015/0223\\_teirei/h26gidai3.pdf](http://www.data.jma.go.jp/gmd/extreme/kaigi/2015/0223_teirei/h26gidai3.pdf)], 2015. 参照 2015-04-27.
  - 5) 気象庁: 気象速報, 平成 26 年 12 月 16~18 日の暴風雪、高波、高潮に関する気象速報（釧路・根室地方）第 1 報 [[http://www.jma-net.go.jp/ku-shiro/tenki/sokuhou/pdf/sokuhou20141216-1218\\_1.pdf](http://www.jma-net.go.jp/ku-shiro/tenki/sokuhou/pdf/sokuhou20141216-1218_1.pdf)], 2014. 参照 2015-03-12.
  - 6) Sunny Spot : SPAS 速報天気図. [<http://www.sunny-spot.net/chart>], 2015. 参照 2015-02-07.
  - 7) 気象庁: 平成 26 年 12 月 17 日に発生した、急速に発達した低気圧による根室地方の高潮に関する現地調査報告（第 2 報（最終報）） [[http://www.jma-net.go.jp/sapporo/oshirase/2015/sp\\_press150116\\_kushiro.pdf](http://www.jma-net.go.jp/sapporo/oshirase/2015/sp_press150116_kushiro.pdf)], 2015. 参照 2015-04-28.
  - 8) 中村亮太, 大山剛弘, 柴山知也, 松丸亮, 高木泰士, Miguel ESTEBAN, 三上貴仁: Typhoon Yolanda によるフィリピンの高潮被災の高潮追算と現地調査の比較, 土木学会論文集 B2 海岸工学, Vol. 70, No. 2, pp. I\_236-I\_240, 2014.
  - 9) Skamarock, W. C., Klemp, J. B., Dudhia, J., Gill, D. O., Barker, D. M., Duda, M. G., Huang, X. Y., Wang, W. and Power, J. G. : A Description of the Advanced Research WRF Version 3. NCAR TECHNICAL NOTE, 2008.
  - 10) Chen C., Liu, H. and Beardsley R. C. : An unstructured, finite-volume, three-dimensional primitive equation ocean model: application to coastal ocean and estuaries, Journal of Atmospheric and Oceanic Technology, Vol. 20, pp. 159-186, 2003.
  - 11) NCAR : NCEP FNL Operational Model Global 2014. Tropospheric Analyses, continuing from July 1999, [<http://rda.ucar.edu/datasets/ds083.2/>]. 参照 2015-01-10.
  - 12) NCAR : Historical Unidata Internet Data Distribution (IDD) Gridded Model Data, December 2002 – current [<http://rda.ucar.edu/datasets/ds335.0>], 2014. 参照 2015-01-10.
  - 13) Davis, C. and Low - Nam. S. : The NCAR - AFWA tropical cyclone bogussing scheme, report, pp.21, U.S. Air Force Weather Agency, Offutt, AFB, Nebr. 2001.
  - 14) Hong, S. Y. and Lim, J. O. J. : The WRF single-moment 6-class microphysics scheme (WSM6). Journal of Korean Meteorological Society Vol. 42, pp.129–151, 2006.
  - 15) Kain, J. S. : The Kain–Fritsch convective parameterization: An update. Journal of Applied Meteorology and Climatology Vol. 43, pp.170–181, 2004.
  - 16) Atkinson, G. D. and Holliday, C. R. : Tropical cyclone minimum sea level pressure/maximum sustained wind relationship for the western North Pacific, Mon. Wea. Rev., Vol. 105, pp.421–427, 1977.
  - 17) 本多忠夫, 光易恒: 水面に及ぼす風の作用に関する実験的研究, 海岸工学論文集, Vol. 27, pp.90-93, 1980.
  - 18) 横田雅紀, 橋本典明, 田中雄太, 児玉充由: うねりを観測する条件での海面抵抗係数の逆推定精度に関する検討, 土木学会論文集B3 海洋開発, Vol.67, No.2, pp.903-907, 2011.
  - 19) GEBCO : [<http://www.gebco.net/>], 2014. 参照 2015-01-07.
  - 20) CGIARCSI : [<http://www.cgiar-csi.org/data/srtm-90m-digital-elevation-database-v4-1>], 2014. 参照 2014-12-25.

#### Field survey and mechanism of storm surge generation invoked by the low pressure with rapid development in Nemuro Hokkaido in December 2014

Ryota NAKAMURA, Takumu IWAMOTO, Tomoya SHIBAYAMA, Takahito MIKAMI, Shunya MATSUBA, Martin MAELL, Akihumi, TAKEKOUJI and Yusuke TANOKURA

The low pressure with rapid development generated storm surge and inundation over a port and city in Nemuro. The aims of this paper are to provide the information of storm surge height measured by the authors and to clarify the generation mechanism of the storm surge. Based on the authors' field survey, the maximum storm surge height at the street and the port in Nemuro was approximately 2.20 m and 2.80 m, respectively. Furthermore, the ground level in Nemuro decreased from coastal line toward the street. According to the numerical results with WRF and FVCOM, the water level in Nemuro bay increased at first because of the East wind. Then, the mass of water intrudes to the Nemuro Peninsula because of north wind and caused the storm surge. In conclusion, the local topography of Nemuro, the direction changes of wind and the topography of Nemuro Peninsula caused the damage of the storm surge to Nemuro.

**Non-exclusive licence to reproduce thesis and make thesis public**

I, Martin Mäll,

1. herewith grant the University of Tartu a free permit (non-exclusive licence) to:
  - 1.1. reproduce, for the purpose of preservation and making available to the public, including for addition to the DSpace digital archives until expiry of the term of validity of the copyright, and
  - 1.2. make available to the public via the web environment of the University of Tartu, including via the DSpace digital archives until expiry of the term of validity of the copyright,
- “Modelling storm surge conditions under future climate scenarios: A case study of 2005 January storm Gudrun in Pärnu, Estonia”,  
supervised by Ülo Suursaar, Ain Kull & Tomoya Shibayama,
2. I am aware of the fact that the author retains these rights.
3. I certify that granting the non-exclusive licence does not infringe the intellectual property rights or rights arising from the Personal Data Protection Act.

Tartu 19.05.2016